INTELLIGENT MOBILE ROBOT FOR PUSHING OBJECTS

A dissertation submitted to the
Department of Electrical Engineering, University of Moratuwa
in partial fulfillment of the requirements for the
degree of Master of Science

By
LEWIS HENNEDIGE JAYATHU DIMUTHU KUMARA FERNANDO

Supervised by: Prof Lanka Udawatta
Co-Supervised by: Dr. Harsha Abeykoon

Department of Electrical Engineering
University of Moratuwa, Sri Lanka

2009

Abstract

In this research, a new approach to develop an object pushing system with a simple mobile robot with two DC servo motor driven wheels and two castor wheels are introduced. This is an attempt to design and develop a system with less number of sensors to detect the reaction force generated on the mobile robot while pushing an object. The robot behavior is such that it always tends to push the object towards the center of the pusher attached to the robot. This is achieved by rotating one driving wheel of the robot by a fixed amount of rotation. This rotation is such that the motor torque is increased continuously by increasing the motor driving positive pulse width of the pulse width modulated signal from its neutral position until the required amount or rotation is obtained. At this moment the motor stops and the wheel attached to the other motor follows the same operation. This motion creates a zigzag movement on the pushing plate attached in front of the robot. This zigzag motion always moves the object towards the centre of the pusher. When the object comes close to the centre of the pusher the force applied from both motors becomes equal. Detection of this force is done by using the positive pulse width of the motor and the encoder pulses generated by the optical encoder attached to both wheels of the robot. The test results are given to support the proposed approach.

DECLARATION

The work submitted in this dissertation is the result of my own investigation, except where otherwise stated.

It has not already been accepted for any degree, and is also not being concurrently submitted for any other degree.

UOM Verified Signature

L.H.J.D.K.Fernando

October 30, 2009

We endorse the declaration by the candidate.

UOM Verified Signature

Prof. Lanka Udawatta

UOM Verified Signature

Dr. Harsha Abeykoon

CONTENTS

Page

Acknowledgement

I would like to express my sincere gratitude to my thesis supervisor Prof. Lanka Udawatta and the co supervisor Dr Harsha Abeykoon for the ingenious commitment, encouragement and highly valuable advice provided to me. Their rigorous attitudes to do the research and inspire thinking to solve problems are invaluable for my professional career.

I would also wish to express my indebtedness to the Arthur C Clarke Institute for Modern Technologies (ACCIMT) for providing me the necessary lab facilities for this research. I wish to thank Mr. Saraj Gunasekara, Head of the Space Applications Division, Mr. Shiran Welikala, Industrial Manager and other colleagues of ACCIMT who helped me in different stages of the project.

Special thanks go to Prof.Nihal Kularatna, senior lecturer of University of Waikato who always encourages me to progress my research work while giving me the necessary advices.

My thanks also go to my beloved mother Karunawathie Silva and late father Wilton Fenando, who bless and encourage me all the time.

My deepest gratitude is also extended towards my family and of course to my beloved wife Chamarie, for her consistent love, support, understanding, encouragement, and for the life we experience together, both in our good times and hard times. Without your support this would never have happened!

Last but not the least; I would like to thank all the staff members of the Department of Electrical Engineering of University of Moratuwa for their great contribution in conducting post graduate course in "Industrial Automation" .

List of Figures

List of tables

Table Page

Chapter 1

1 Introduction

Manipulation of an object when it is moving from one place to another is one basic task of a robot. With some flexible manipulators the object can be gripped, picked up and placed at any required position. When the object is too large, too heavy or complex to be gripped this method can no longer be utilized to move an object. Hence any sort of a nonprehensile manipulation has to be used. Pushing is a very much suitable alternative in this type of situation. It does not require a special grasping tool, manipulator to lift and support the work pieces.

There are several issues needed to be considered when an object is been pushed by a mobile robot (MR). Some of those factors are listed below.

- Shape of the object
- The properties of the terrain which the object is being pushed.
- Friction between the terrain and the object
- Friction between the terrain and the mobile robot.

The object consist of a surface which does not get stuck on the floor while it is pushing. If the object gets stuck on the floor there is a necessity of applying a considerable large force on the object either to take it out of the place where it stucks or turn the object around that point.

The amount of the object that is sunk into the terrain is also very important. This is depending on the properties of the terrain and the weight of the object. If the terrain is having low dense soil or material it is hard to push the object. The movement of the mobile robot also becomes difficult in this type of terrains. The inclination of the terrain to the horizontal plane of the earth is also a very important factor. If the object

is moving on a surface which climbs up, it is hard to push the object. On the other hand it is easy to push an object downwards. But the object is having a tendency to roll down along the terrain at this instance. If rolling occurs it is hard to monitor the object. So it becomes complex and have to use sensors to monitor the object.

This property of the terrain also leads to the friction force between the terrain and the object and that of the terrain and the mobile robot. Moving an object along a smooth surface needs less force than on a rough surface. Since the friction force between the terrain and the robot also changes with the roughness of the terrain slipping may occur on the wheels of the mobile robot.

1.1 Objective

When an object needs to be moved by pushing, there are lots of factors needed to be considered. One factor is the shape of the object. Another factor is the center of friction (COF) of the object that has to be moved. If we can identify the COF of the object we need to apply the force through a line which passes through the COF. If the terrain is homogeneous, the shape of the object is symmetrical and having equal density throughout the object, it is easy to find the COF of the object using image processing techniques. But it is very difficult to find the COF if the object and terrain does not satisfy the above properties.

The objective of this research is to push any shaped object which can be pushed on a terrain, with approximately equal torque on both left and right side motors of the mobile robot. This condition occurs when the COF of the pushing object lies on the symmetrical plane of the MR. The pulse width modulated waveforms used to drive the servo motors and the output of the optical encoder attached to the wheels are the only parameters used to achieve the above task. Only the torque exerted on each motor is used to find the force applied on the object and the output of the optical encoder attached to each wheels is used to get the distance travelled by each wheel. The combination of maximum motor driving torque of each wheel and the moving distance of each wheel is used to get the force applied on the object.

1.2 System Design

The MR base is constructed with a 1cm thick fiber platter. Two caster wheels are attached as the front wheels and two other wheels attached with Futaba servo motors are fixed as the back of the above mentioned platter. Two encoder wheels are attached to both driving wheels. Photo reflector ICs attached to the base, close to the wheel encoder are used to read the encoder pulses generated by white color grooves on the black color encoder wheel. A 30cmX12cm plate made out of MDF board is attached in front. This plate acts as a pushing bar. Controlling the two DC servo motors and reading the encoder pulses are the main tasks of the main controller circuit specially designed for this MR.

1.3 Background of Previous Research

In 1986 Mason[1] first presented research results on pushing a solid object by a manipulator. In his research he analyzed the mechanics of quasi-static pushing operations. This analysis showed the algorithm to determine the rotation direction (clockwise, counter clockwise) of a pushed object, when the pressure distribution is unknown. He showed that the moving object by actively pushing with a manipulator is also flexible and mechanically less complex than pick- and-place, for planer positioning. This process does not require a special grasping tool and the manipulation lift is also not a must. In 1998 Brost[2] utilized the results of Mason[1] to develop an analysis of grasping action with parallel jaw grippers. He analyzed the possible motion of an object being pushed by a fence to obtain the Push Stability Diagram too. Mani and Wilson[3] used the Mason's rules to derive an Edge Stability Map which was used to orient polygonal objects. Peshkin and Sanderson [4][5] extended this analysis of pushing by attempting to solve the motion of the pushed object completely. The pushing operation has been utilized in many applications after these results obtained through the previous researches. Akella and Mason [6][7] studied the use of pushing action to move any polygonal object from any initial configuration to any

final configuration. Lynch et. al.[8] studied the problem of transferring a part from one state to another using nonprehensile manipulation. This research includes the quasistatic nonprehensile manipulation and the dynamic nonprehensile manipulation. Agarwal.et. al. [9] considered the path-planning problem for a robot pushing a unit disk with point contact in an obstacle free environment. Besides these open-loop designs of pushing operation series, many researchers have studied the feedback control of the object pushed by robots. Takagi et. al. [10] took the rule-based control scheme to control a mobile robot pushing a box, based on their analysis of the moving equations of the robot and box. Okawa et. al. [11] resolved the same problem with the goal seeking strategy for robot's motor control. Lynch and Kevin [12] developed a control system to translate and orient objects using tactile feedback with the derived motion equations of the pushed objects.

1.4 Outline of Thesis

The remaining part of the thesis is made up as follows.

Chapter 2 deals with the basic requirements and theories needed to be considered when an object is under push. This chapter describes the different types of frictional forces and force diagram of the object. Chapter 3 contains the details of the new technique used to find the center of friction of an object (COF) using the motor driving parameters and encoder output of the MR. It also describes the mechanism of getting the object to the middle of the pushing plate attached to the MR. Chapter 4 deals with the development of MR. This chapter contains all the technical details of each and every part used to develop the MR. The new method of driving 50Hz PWM controlled dc servo motors using the 250Hz PWM output of a PIC microcontroller are also described in this chapter. Chapter 5 shows the result obtained in the new implementation. Chapter 6 deals with the conclusions, some suggested modifications and recommendations.

Chapter 2

2 Fundamentals of pushing object

Most objects are at rest most of the time. To move an object a force is needed to be applied on it. There are two frictional contacts needed to be addressed when moving an object. One is the friction between the terrain and the object. The other is the friction between the moving object and the pusher.

2.1 Coulomb's Law

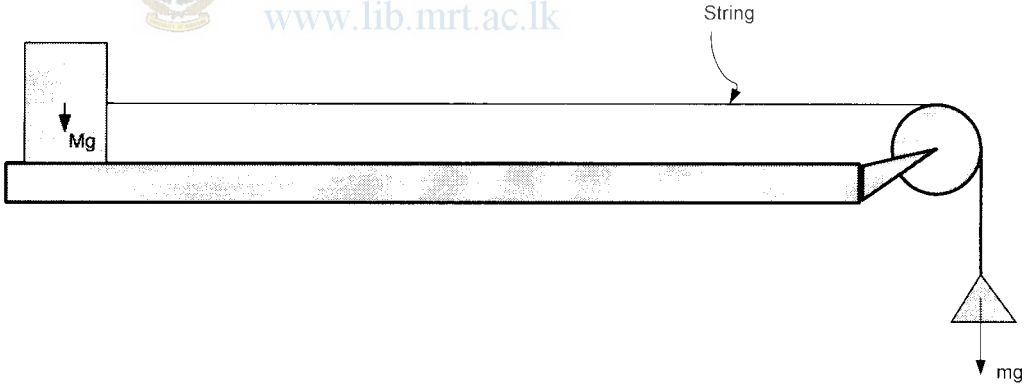

Figure 2-1: Test for friction force

Consider a block sliding on a horizontal surface, pulled by a string as shown in figure 2-1. Assume the two surfaces are fairly clean, dry, and unlubricated. Imagine that the instruments are available to measure the force f_a applied via the string, and the tangential force f_f due to friction between the table and the block. If the applied force

f_a increased gradually, the behavior illustrated in figure 2-2 can be observed. For small applied forces, the frictional force will balance the applied force, so that the block does not move. Above some threshold, the block will begin moving, and the frictional force will now be constant. If a large number of experiments are carried out by varying the block's mass, the block's shape, the materials, and so forth, the factors for the limiting frictional forces can be identified as the normal force, and the materials involved. If f_{ts} is the limiting value of static friction, at which motion begins, and f_{td} is the value of dynamic friction, then these values are approximately:

$$f_{ts} = \mu_s f_n$$

$$f_{td} = \mu_d f_n$$

Where f_n is the normal force, μ_s is the static coefficient of friction, and μ_d is the dynamic coefficient of friction. Typically μ_s is larger than μ_d, but this difference is ignored and speak of a single coefficient of friction μ. A simple statement of Coulomb's law is:

$$|\boldsymbol{f}_t| \leq \mu |\boldsymbol{f}_n|$$

if there is no motion, and if there is any motion, with the tangential force in a direction opposite to the motion.

$$|\boldsymbol{f}_t| = \mu |\boldsymbol{f}_n|$$

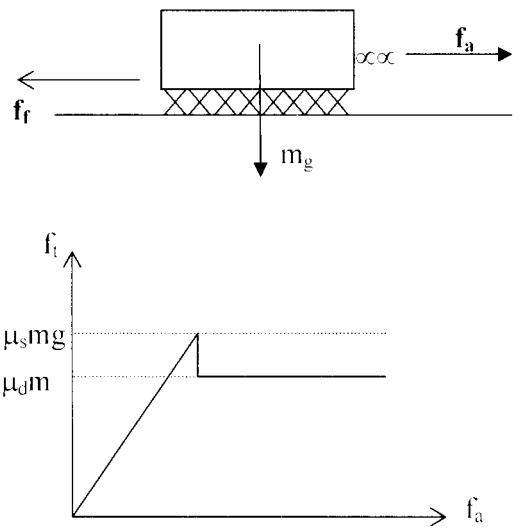

Figure 2-2 Coulomb's law of sliding friction

In particular, the tangential force is largely independent of the contact area, and of the velocity of motion. The coefficient of friction is considered to be a material property, depending only on the materials involved. Tables of the coefficient of friction should not be taken too seriously, but some typical values are given below:

Table 1: The friction coefficient between some materials

Materials	μ
metal on metal	0.15-0.6
rubber on concrete	0.6-0.9
plastic wrap- on lettuce	∞
Leonardo's number	0.25

Experiments like those described above provide the basis of Coulomb's law, which will be stated more carefully later. The history of the law is also interesting. Coulomb's work with friction was his first scientific achievement. Coulomb's interest in friction was spurred by practical engineering matters. He was a military engineer in carrier and carried his huge laboratory apparatus with him from one assignment to another. Coulomb is also known for the invention of the torsion balance and for his studies of electricity, leading to the law for electrostatic attraction which is unfortunately also known as Coulomb's law.

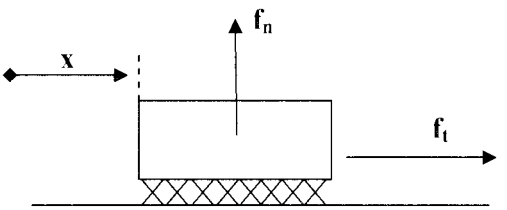

Figure 2-3 Sliding block with Coulomb friction

Coulomb was not the first to propose Coulomb's law of sliding friction. Amontons had proposed it earlier, and the law is occasionally referred to as Amontons's law. It also appears that Leonardo da Vinci had earlier posed a more restrictive version of the law, supposing the coefficient of friction to be always one fourth. Coulomb's law is a phenomenological law, providing an approximate description of an aggregate behavior. For that reason there are some who would prefer not to call it a law at all. There are more fundamental approaches to the modeling of friction, and more precise approximations of friction. But Coulomb's law still provides the best combination of simplicity and accuracy for many purposes.

2.2 Single degree-of-freedom problems

Lets begin by considering the simplest problems, involving just one degree of freedom. Consider a block in frictional contact with a supporting plane, which is prevented somehow from moving away from the plane (fig. 2-3). The tangential position of the block is given by x, and the frictional force is given by f_n and f_t, respectively normal and tangential to the supporting plane. Coulomb's law prescribes a constraint on the contact force, depending on the *contact mode* indicated in the table2

Table 2: Contact force and contact mode

$\dot{x}$	$\ddot{x}$		
< 0		$f_t = \mu f_n$	left sliding
> 0		$f_t = -\mu f_n$	right sliding
$= 0$	<0	$f_t = \mu f_n$	left sliding
$= 0$	>0	$f_t = -\mu f_n$	right sliding
$= 0$	$=0$	$\lvert f_t \rvert \leq \mu f_n$	rest

Now suppose that a gravitational field is introduced. So that the supporting surface is an inclined plane (fig. 2-4). Let α be the angle of the inclined plane with respect to the horizontal. What is the maximum angle α at which the block can remain at rest?

If the block is at rest, then the gravitational force must balance the total contact force:

$$f_n = mg\cos\alpha$$

$$f_t = mg\sin\alpha$$

At rest we have $|f_t| \leq |\mu f_n|$. The limiting case is given by

$$f_t = \mu f_n$$

Substituting,

$$mg\sin\alpha = \mu mg\cos\alpha$$

$$\alpha = \tan^{-1}\mu$$

The desired angle α is the arc-tangent to the coefficient of friction. This angle is sometimes called the friction angle or the angle of repose.

The friction angle provides an elegant geometrical approach to Coulomb's law. Consider all the forces satisfying Coulomb's law for an object at rest, i.e. all the forces satisfying the condition

$$|f_t| \leq |\mu f_n|$$

This set of forces describes a cone in the force space, called the *friction cone*, with vertex at the origin, and dihedral angle $2\tan^{-1}\mu$ (fig.2-4). Then Coulomb's law can be stated as

For left sliding $\quad f_n + f_t \in$ right edge of friction cone

For right sliding $f_n + f_t \in$ left edge of friction cone

For rest $f_n + f_t \in$ friction cone

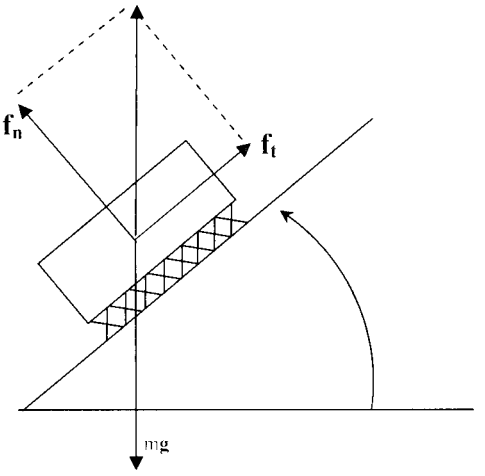

Figure 2-4 Sliding block on inclined plane

.

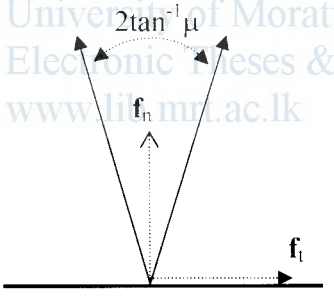

Figure 2-5 The friction cone

To satisfy Coulomb's law the contact force deviates by at most $\tan^{-1}\mu$ from the contact normal.

2.3 Planar sliding

Some manipulation tasks involve an object sliding on a planar support surface. The motion of a pushed object is often undefined. If a rigid object is supported by more than three contact points, the distribution of supporting forces are underdetermined. If the frictional forces are assumed proportional to the normal forces, as Coulomb suggests, then the frictional forces are also underdetermined. The problem is illustrated by the defective dinner plate of fig.2-6. The plate was designed with a circular ridge on the bottom, so that the supporting forces would be concentrated at the edge of the plate. Unfortunately, the bottom of the plate sagged during the firing process, so that the center is also in contact with the planar support. There is no way to predict whether the support forces will be concentrated at the center, giving it an irritating tendency to rotate, or at the edge, resisting rotation. In practice, the plate's behavior will depend on details that may be very difficult to model. It may behave well with a tablecloth, and poorly without a tablecloth. Its behavior might depend on the phase of the moon. (Tidal forces induce microscopic changes in the shapes of the plate and table.)

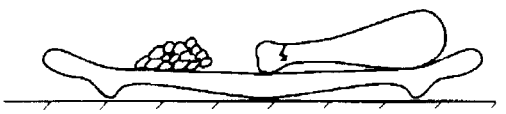

Figure 2-6 Cross section of a plate

It is impossible to predict the motion of this plate, without knowing the distribution of supporting forces between the plate and the table.

2.4 Force and moment of planar sliding

Let some object be in planar motion, supported by a fixed planar surface. Choose a coordinate frame with the *x*-*y* plane coincident with the support, and *z* pointing outward. Let the object's contact with the surface be confined to some region *R*. Let **r** be the position vector of some point in the object, and let ***v(r)*** be the velocity of that point.

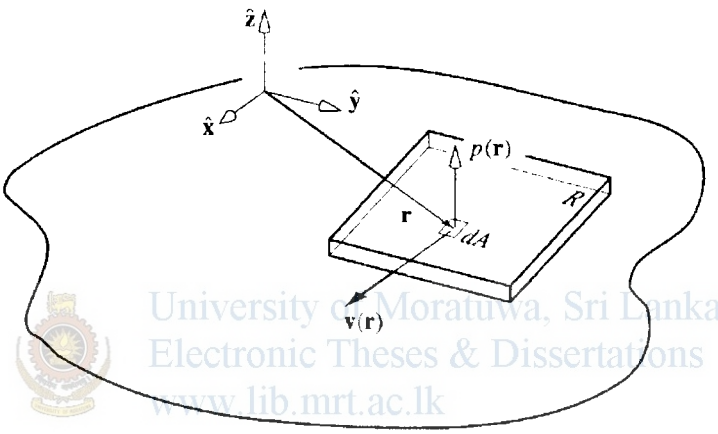

Figure 2-7 Notation for planar sliding.

If $p(\boldsymbol{r})$ is the pressure at **r**, and dA a differential element of area at **r**, then the magnitude of the normal force at **r** is given by

$$p(\boldsymbol{r})dA$$

and Coulomb's law gives us the tangential force at **r**:

$$-\mu\frac{\boldsymbol{v}(\boldsymbol{r})}{|\boldsymbol{v}(\boldsymbol{r})|}p(\boldsymbol{r})dA$$

for $|\mathbf{v}(\mathbf{r})| \neq 0$, where μ is the coefficient of friction, assumed uniform over the contact region R.

Integrating over R, we obtain expressions for the total force and moment due to friction:

$$\boldsymbol{f}_f = -\mu \int_R \frac{\boldsymbol{v}(\boldsymbol{r})}{|\boldsymbol{v}(\boldsymbol{r})|} p(\boldsymbol{r}) dA \qquad \rightarrow 2.1$$

$$\boldsymbol{n}_f = -\mu \int_R \boldsymbol{r} \times \frac{\boldsymbol{v}(\boldsymbol{r})}{|\boldsymbol{v}(\boldsymbol{r})|} p(\boldsymbol{r}) dA \qquad \rightarrow 2.2$$

Note that the frictional force $\mathbf{f}_f$ lies in the x-y plane; and the total frictional moment $\mathbf{n}_f$ acts along the z-axis. Without knowledge of the pressure distribution $p(\boldsymbol{r})$, these integrals cannot be evaluated, leading to indeterminacy in the frictional forces. There is an exception, though: pure translation.

2.4.1 Case 1: Pure translation

If the object is in pure translation, all points are moving in the same direction, and we can factor the integrals of equations 2.1 and 2.2.

$$\boldsymbol{f}_f = -\mu \frac{\boldsymbol{v}(\boldsymbol{r})}{|\boldsymbol{v}(\boldsymbol{r})|} \int_R p(\boldsymbol{r}) dA \qquad \rightarrow 2.3$$

$$\boldsymbol{n}_f = -\mu \int_R \boldsymbol{r} p(\boldsymbol{r}) dA \times \frac{\boldsymbol{v}(\boldsymbol{r})}{|\boldsymbol{v}(\boldsymbol{r})|} \qquad \rightarrow 2.4$$

Let $\mathbf{f}_0$ be the total normal force, and let $\mathbf{r}_0$ be the centroid of the pressure distribution.

Then

$$f_0 = \int_R p(\boldsymbol{r})dA$$

$$\boldsymbol{r}_0 = \frac{1}{f_0}\int_R \boldsymbol{r}p(\boldsymbol{r})dA$$

Substituting into equations 2.3 and 2.4,

$$\boldsymbol{f}_f = -\mu\frac{\boldsymbol{v}(\boldsymbol{r})}{|\boldsymbol{v}(\boldsymbol{r})|}f_0$$

$$\boldsymbol{n}_f = \boldsymbol{r}_0 \times \boldsymbol{f}_f$$

Hence the frictional forces distributed over the supporting region have a resultant, with magnitude μf_0, in a direction opposing the motion, through the centroid $\mathbf{r}_0$. In other words, the force is equivalent to that obtained by applying Coulomb's law to the sliding of a single point located at $\mathbf{r}_0$.

(The center of friction (COF) is the centroid $\mathbf{r}_0$ of the pressure distribution.)

In some cases, the center of friction is easily determined. If an object is at rest on the supporting plane, with no applied forces other than gravity and the supporting contact forces, then the center of friction is directly below the center of gravity. This is the only location that allows the contact forces to balance the gravitational force. We can generalize slightly, allowing additional applied forces, as long as they are in the supporting plane. We can also permit accelerated motion of the body, if the center of gravity is in the supporting plane. But acceleration of a body whose center of gravity is above the supporting plane it will in general, cause a shift in the pressure

distribution, and a corresponding shift in the center of friction. Applied forces not lying in the supporting plane will generally cause a similar shift.

2.4.2 Case 2: Rotation

Now suppose that the body is rotating, with an instantaneous center r_c. Then the velocity of a point at r is given by

$$\boldsymbol{v}(\boldsymbol{r}) = \boldsymbol{\omega} \times (\boldsymbol{r} - \boldsymbol{r}_c)$$

$$= \dot{\theta}\hat{\boldsymbol{k}} \times (\boldsymbol{r} - \boldsymbol{r}_c)$$

and the direction of motion at **r** is

$$\frac{\boldsymbol{v}(\boldsymbol{r})}{|\boldsymbol{v}(\boldsymbol{r})|} = sgn(\dot{\theta})\hat{\boldsymbol{k}} \times \frac{(\boldsymbol{r} - \boldsymbol{r}_c)}{|\boldsymbol{r} - \boldsymbol{r}_c|}$$

Substituting into equations 2.1 and 2.2 we obtain

$$\boldsymbol{f}_f = -\mu\, sgn(\dot{\theta})\hat{\boldsymbol{k}} \times \int_R \frac{(\boldsymbol{r} - \boldsymbol{r}_c)}{|r - r_c|} p(\boldsymbol{r}) dA$$

$$n_{fz} = -\mu\, sgn(\dot{\theta}) \int_R \boldsymbol{r} \,.\, \frac{(\boldsymbol{r} - \boldsymbol{r}_c)}{|\boldsymbol{r} - \boldsymbol{r}_c|} p(\boldsymbol{r}) dA$$

These equations have a well-defined limit as the rotation center $\mathbf{r}_c$ approaches infinity, so they apply to pure translations as well as rotations.

3 Methodology of finding Centre of Friction of an Object

In order to push an object with a MR comfortably the object should make approximately equal reaction on the wheels on both sides of the robot. Hence the COF of the object should be kept on the Symmetrical plane of the MR. So there should be a method to find the COF of the object. If the shape of the object is arbitrary and the terrain where the object is being pushed is not even, finding of the COF is not an easy task. Centre of mass of an object with a known shape can be found by using an image processing technique if the mass distribution inside the object is even.

In this research only the servo motor driving PWM waveform and the encoder pulses are used to determine the COF of any shaped object.

3.1 Forces act on moving object

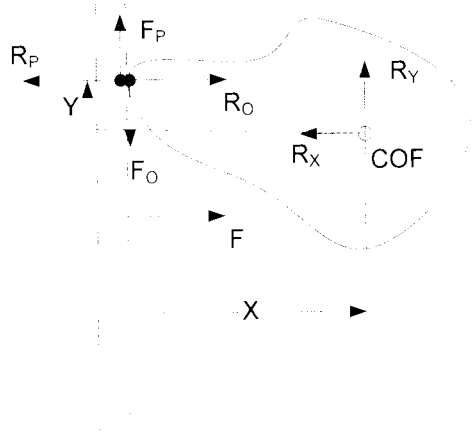

Figure 3-1 Forces act on pusher and the object

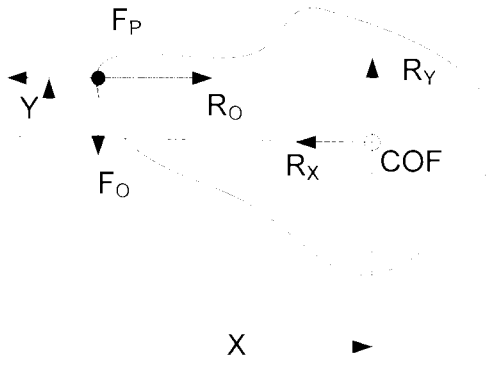

Figure 3-2 Forces act on the object

Where

R_x	Reaction on the object from the floor along x axis
R_Y	Reaction on the object from the floor along y axis
R_O	Reaction force on the object
F_O	Friction force on the object from the plate
R_P	Reaction force on the plate
F_P	Friction force on the plate from the object
X	Distance between COF and the plate perpendicular to R_O
Y	Distance between COF and touching point perpendicular to F_O
F	Force applied on the plate

If an object is being pushed by a plate as shown in figure 3.1 there are several reactions needed to be considered to predict the movement of the object. When the object and its touching point of the plate are considered,

$$R_O = R_P$$

$$F_O = F_P$$

If these forces are at equilibrium

$$R_O = R_P = R_X = F$$
$$F_O = F_p = R_Y$$

$$F_O * X = R_O * Y$$

$$F_O = \mu_{op} R_O$$

$$R_X^2 + R_Y^2 = \mu_f Mg$$

Where M is the mass of the object

g is the gravitational acceleration

μ_{op} is the friction coefficient between the plate and the object

μ_f is the friction coefficient between the floor and the object

When the force applied from the plate increased this equilibrium will break and object starts to move and rotate. If the F_O is greater than maximum possible static friction force the object tries to slip along the plate. Due to the torque created by $(F_O \hat{} X - R_O \hat{} Y)$ the object tries to rotate around the COF. Direction of this rotation depends on the magnitudes of F_O, R_O and the distance between the COF of the object and the plate. This rotation will stop when the object rotates to a position which creates zero torque around the COF of the object. At this stage the object might touch the plate from several points. Figure 3-3 shows such arrangement of an object. Here the R_{Oi} and

F_{Oi} are the reaction and friction forces on the object at the i^{th} point of contact. Hence this arrangement can mathematically be represented as follows

$$\sum_{i=1}^{n} F_{Oi} \hat{} X_i - \sum_{i=1}^{n} R_{Oi} \hat{} Y_i = \text{Total torque on the object in clockwise direction}$$

Here the Xi and Yi are the distance from COF to F_{Oi} and R_{Oi} respectively and n is the number of touching points of object and the pusher. If this torque is zero then there is no rotation of the object.

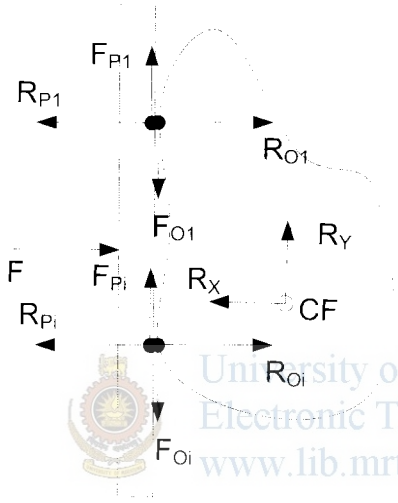

Figure 3-3. Several points of contact between plate and the object

Similarly if the $R_X^2 + R_Y^2$ is greater than the maximum allowable static friction force between the object and the floor, the object tends to moveto the direction of the applied force. If the force applies on the object changes its direction there is a possibility of passing the applied force through the COF of the object. At that instance the object will only move towards the direction of the applied force without any rotation.

When an object is being pushing, we need to keep COF of the object closer to the centre of the pushing bar. Then equal torque applies to both motors. So the object needs to be pushed to the centre of the pusher if it is in a side of the pusher. Since the

pusher creates both rotational motion around the COF of the object and perpendicular motion along the COF of the object when pushing with higher force by turning the angle between the pusher and the object the object can be moved towards the centre of the pusher. This action need to be done by both sides of the pusher. Then the robot tends to move in a zigzag pattern. This zigzag pattern can be implemented by turning one wheel of the MR at a time.

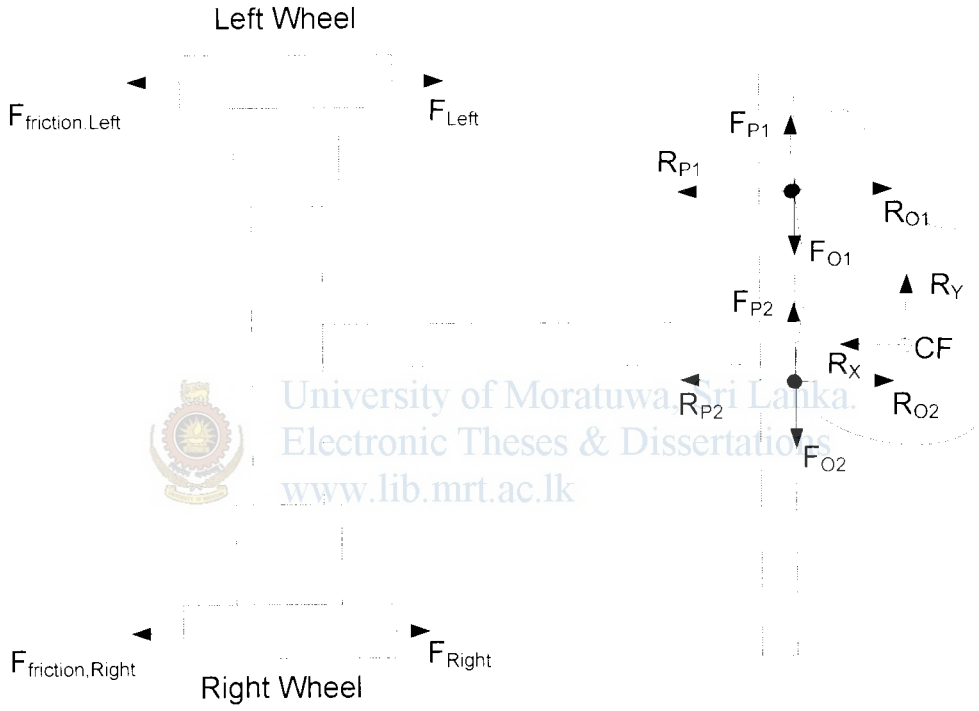

Figure 3-4 Forces applied on Mobile robot

If an object is being pushed by a plate as shown in figure 3-4 there are several reactions needed to be considered to predict the movement of the object. When the object and the touching point of the plate are considered, a reaction force creates due to friction on the object. The magnitude of this force mainly depends on the weight of the object and the frictional force created on the object.

3.2 Zigzag movement of the robot and detection of the COF of the object

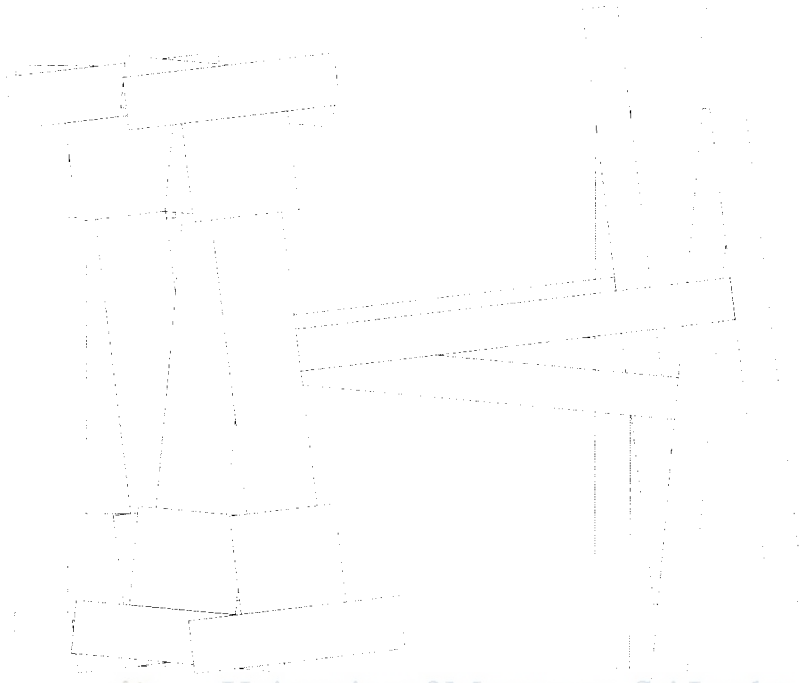

Figure 3-5 Zigzag Motion of the Mobile Robot

As shown in the figure 3-5 the robot moves turning one wheel at a time. The wheel speed is increased from its neutral position by changing the pulse width of the DC servo motor input. This is done while monitoring the encoder pulses produced by the encoder attached to the rotating wheel. In every 20ms the positive width of the PWM signal is increased by 4us and this will create more and more force on the motor. When the motor torque is sufficient to move the MR the robot will start to turn. Still the PWM positive width increment is going on. When the pusher attached to the MR touches an object the speed of the MR get slower. If it touches close to the driving motor side edge of the pusher the motor needs more power to drive it. Hence motor speed gets much slower. Then it needs more time to rotate the wheel until it produces the required number of pulses. But the object moves more towards the centre. When the required number of encoder pulses are obtained the motor stops it's rotation and will record the maximum positive pulse width used to drive the motor. After that the

motor attached to the other side starts applying the positive pulse width in the same way as the other side motor. When wheel encoder gives the required number of pulse this motor also stops and will record the maximum pulse width used to drive this motor. This process continues until both motors produce the same maximum pulse width. Since the zigzag motion produces motion of the object towards the centre of the pusher the object will never escape from the pusher once it touches firmly.

4 Development of the Mobile Robot

Mobile robot is the most important part of the whole project. It will move according to the instruction provided to it from remote computer. While it is traveling it pushes the object along its path and tries to get the object to the centre of the pusher attached to it on front side. Hard and low weighting fiber platter is the basic platform of the mobile robot and the other items are mounted on it. The movement of the robot is done by using two servo motors attached with the two driving wheels. Two castor wheels mounted in front of the robot platter adjust its orientation according to the rotation of two driving wheels. When the robot is turning the amount of rotation of the two driving wheels is extremely important. Two optical encoders attached to the driving wheels provide that information in the form of pulses. All the functions of the mobile robot are controlled by the controller board which is designed using PIC micro controllers. Figure 3.1 shows the platter, two driving wheels and two castor wheels arrangement for the mobile robot.

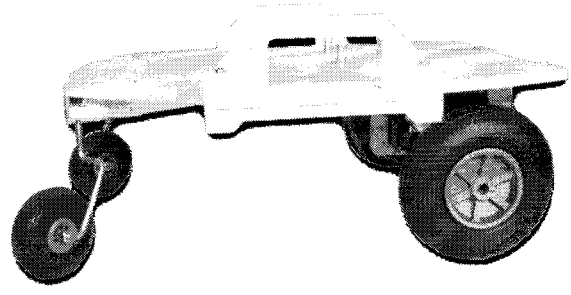

Figure 4-1 Basic mobile robot platform

4.1 The DC Servo motors

Figure 4-2 shows an image of the FUTABA S3104 DC servo motor. Lower image shows the set of gear wheels mounted inside the enclosure. Two of these DC servo motors are attached with two rubber wheels providing the moving capability of the robot. This DC servo motor is operated by 5V DC voltage and PWM (Pulse Width Modulation) signal of 50 Hz. A pulse width of 20 ms time period and an on-time of 1500 μs will stop the rotation of the motors. If the on-time of the pulse is decreased from 1500 to 1000 us the wheel rotates with increasing velocity in the clockwise direction. Similarly if the on-time of the pulse is increased from 1500 to 2000 μs the wheel rotates with increasing velocity in the anticlockwise direction. This motor produces 9.2kg.cm of maximum torque at 4.8V.The positive pulse width which keeps the motor stand still can change by turning the preset which is mounted under the wheel mounting shaft. This preset value can be changed by inserting a small screw driver through the hole on the shaft. This will help to have both motors operated at the same speed at the same positive width.

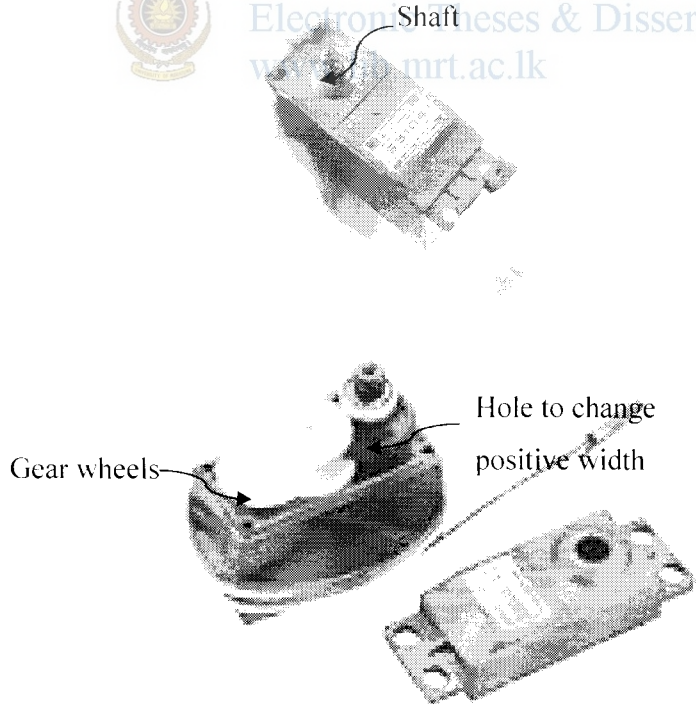

Figure 4-2 Futaba S3104 DC servo motor

Figure 4-3 shows the arrangement of two DC servo motors and the driving wheels in the robot platform. The fiber platter has a special slot for mounting the DC servo motors. Rubber wheels are coupled with the DC servo motor using a screw passing through the center of the wheel.

Figure 4-3 Rubber wheels and DC servo motors assembling

Two castor wheels are mounted on the opposite corners of the plastic base. They are free to rotate as the robot unit moves. Figure 4-4 shows the two caster wheels.

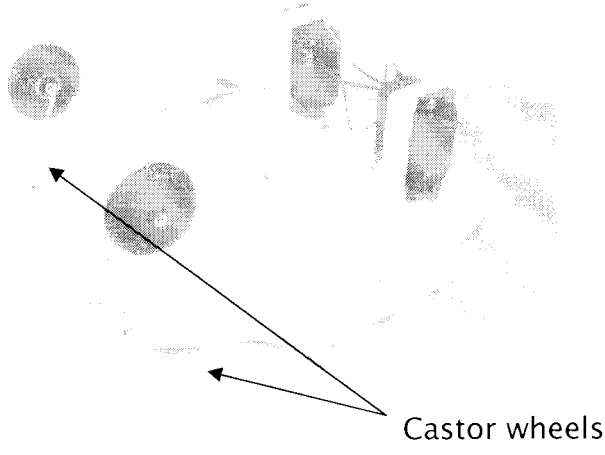

Figure 4-4 Castor wheels and two servo motors

4.2 Driving of the FUTABA S3104 DC servo motor

To drive the FUTABA S3104 DC servo motors there is a necessity of generating PWM waveforms. This waveform should have a frequency of 50Hz (period of 20ms) to drive the DC servo motor. On the other hand the positive pulse width of the waveform should vary in between 1ms to 2ms for changing the speed and direction of the rotation. 1.5 ms of positive width keeps the DC servo motor in a stand-still position. When there is no external load applied, 1.5ms to 1ms positive width variations drive the motor in one direction while increasing the rotational speed from 0 rpm to 40rpm and the 1.5ms to 2ms positive width variations turns the motor to the opposite direction from 0 rpm to 40rpm. The Figure 4-5 shows the minimum & maximum pulse width changing from the 1.5ms neutral position.

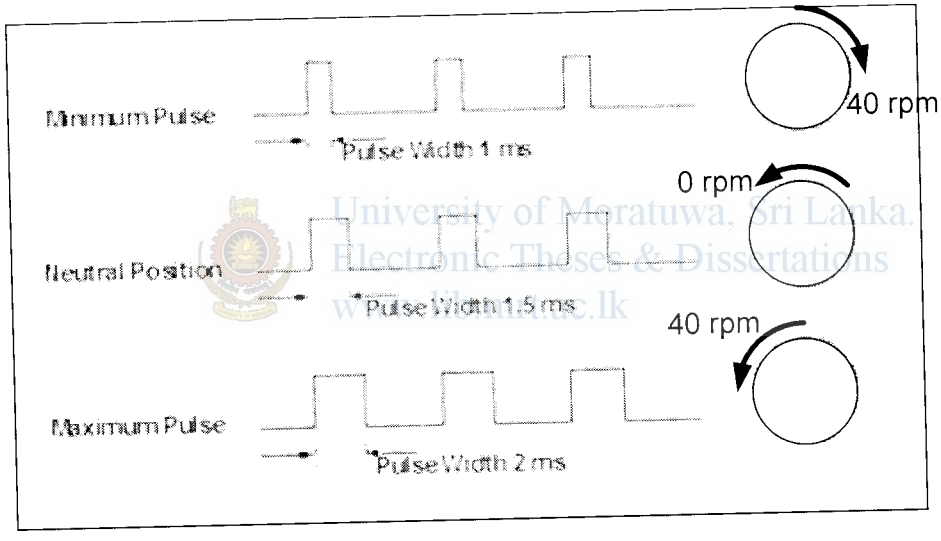

Figure 4-5 Change of the servo Speed with PWM Positive width

4.3 Generation of PWM waveforms

PWM modules of the PIC16F876 microcontroller are used to drive two DC servo motors of the robot. Since the DC servo motor driving PWM should have a frequency of 50Hz, there is a difficulty in the waveform production directly by the PIC

microcontroller. With a 4MHz driving clock (Tosc) the minimum frequency of the PWM output that microcontroller can produce is 244Hz.This problem was solved with the help of a special digital circuit design.

4.3.1 PWM modules of the PIC16F876

PIC 16F876 consists of two PWM modules. In PWM mode, these PWM modules will produce up to 10-bit resolution PWM output. Figure4-6 shows a simple block diagram of a PWM module. It shows the PR2 register which used for generating the period of the waveform.CCPR1L and CCPR1H are used for positive width generation.

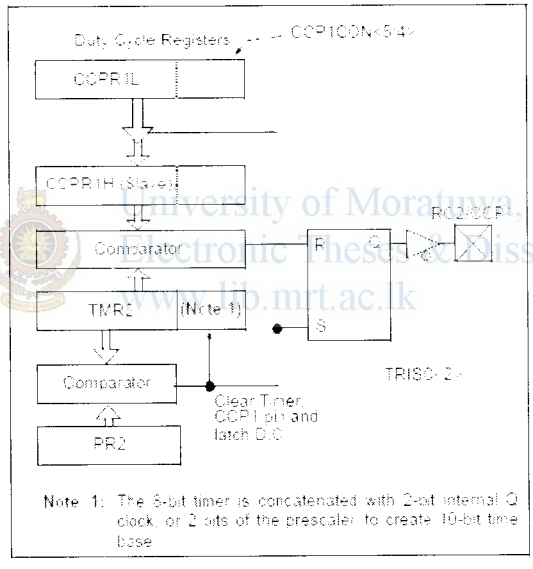

Figure 4-6 diagram of the PWM module of PIC microcontroller

4.3.2 PWM Period

The PWM period is specified by writing to the PR2 register. The PWM period can be calculated using the following formula:

$$\text{PWM Period} = \{(PR2\ Value) + 1\} * 4 * Tosc * (TMR2\ Prescale\ Value)$$

$$PWM\ frequency = \frac{1}{PWM\ Period}$$

When TMR2 is equal to PR2, the following three events occur on the next increment cycle:

- TMR2 is cleared
- The CCP1 pin is set (exception: if PWM duty cycle = 0%, the CCP1 pin will not be set)
- The PWM duty cycle is latched from CCPR1L into CCPR1H

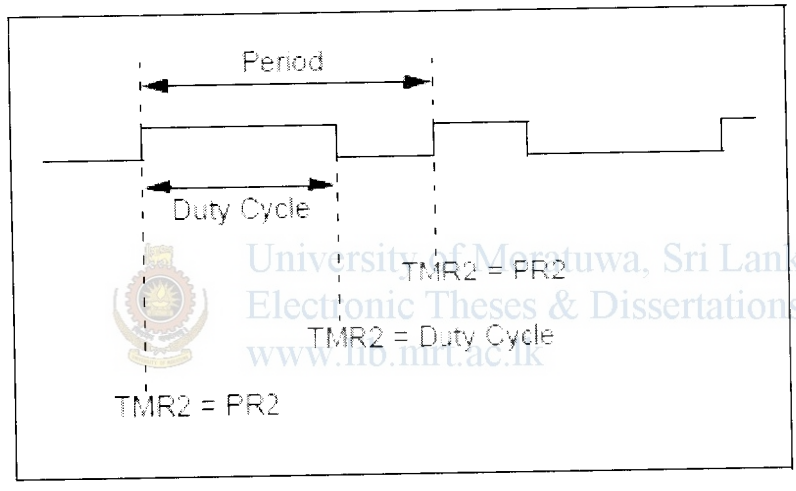

Figure 4-7 Register values at transition point of PWM waveform

4.3.3 PWM duty cycle

The PWM duty cycle is specified by writing to the CCPR1L register and to the 4th and 5th bits of the CP1CON register (CCP1CON<5:4>). Up to 10-bit resolution is available. The CCPR1L contains the eight MSbs and the CCP1CON<5:4> contains

the two LSbs. This 10-bit value is represented by CCPR1L:CCP1CON<5:4>. The following equation is used to calculate the PWM duty cycle in time:

$$\text{PWM Duty Cycle} = (\text{CCPR1L:CCP1CON} < 5:4 >) * \text{Tosc} * (\text{TMR2 Prescale Value})$$

CCPR1L and CCP1CON<5:4> can be written to at any time, but the duty cycle value is not latched into CCPR1H until after a match between PR2 and TMR2 occurs (i.e., the period is complete). In PWM mode, CCPR1H is a read-only register. The CCPR1H register and a 2-bit internal latch are used to double-buffer the PWM duty cycle. This double-buffering is essential for glitch-free PWM operation. When the CCPR1H and 2-bit latch match TMR2, concatenated with an internal 2-bit Q clock or 2 bits of the TMR2 prescaler, the CCP1 pin is cleared. The maximum PWM resolution (bits) for a given PWM frequency is given by the following formula.

$$Resolution = \frac{\log\left(\frac{Fosc}{F_{PWM}}\right)}{Log(2)}\ bits$$

4.3.4 Setup of CCP module for PWM operation

The following steps should be taken when configuring the CCP module for PWM operation:

1. Set the PWM period by writing to the PR2 register.
2. Set the PWM duty cycle by writing to the CCPR1L register and CCP1CON<5:4> bits.
3. Make the CCP1 pin an output by clearing the TRISC<2> bit.
4. Set the TMR2 prescale value and enable Timer2 by writing to T2CON.
5. Configure the CCP1 module for PWM operation.

4.4 Generation of the 50Hz PWM signal using the 250Hz PWM output of the PIC microcontroller.

The minimum output frequency which the PWM module of PIC microcontroller can generate with a 4MHz oscillator is 244Hz. So 250Hz PWM signal was generated by writing the corresponding value to the PR2 register. A 10 bit digital counter (HEF4017) is fed with this 250Hz signal. The counter made reset using the 5^{th} output pin. So the each output pins, pin0 to pin5 of the decade counter will produce a rectangular waveform with 20ms positive width. When the 20ms signal and the input signal fed to two inputs "AND" gate the output is only one cycle out of five cycles of the 250Hz PWM output. The positive width variation required to drive the DC servo motor is between 1ms to 2ms.This variation can be obtain with the output of the above circuit and the PWM duty cycle change of the microcontroller. The propagation delay of the HCF4017 of SGS Thomson Microelectronic[14] is about 325ns at 5V and that of an AND gate of Fairchild Semiconductor Corporation[17] is less than 20ns.So this generated a small pulse at the output of the U1 and U3.To rectify this issue two 100nf capacitors connected between ground and the U1 and U3 outputs. Then the shape of the required PWM pulse shows a small distorted shape at the edges. So these two waveforms are again sent through two AND gate as shown in the Figure 4-8. Then the U2 and U4 output generated the required PWM waveform which needs to drive the DC servo motors.

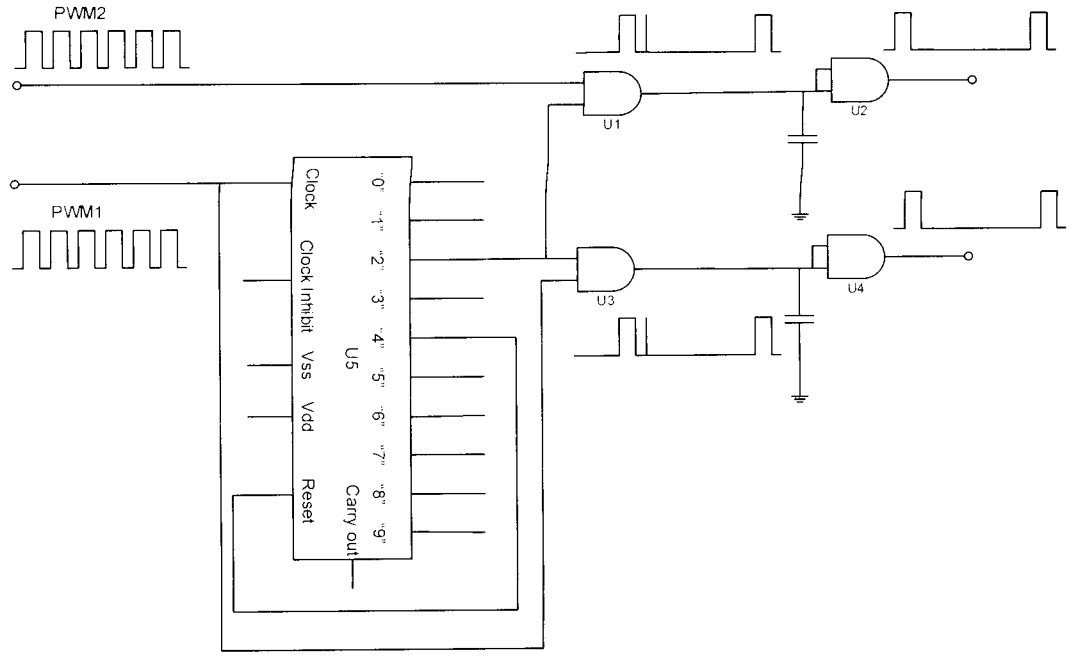

Figure 4-8 Circuit diagram of 50Hz PWM output from 250Hz PWM waveform

4.5 The Optical encoders

The encoder wheels have white colour slots on black colour wheels. This encoder wheels are attached to the driving wheels to detect the rotation. HAMAMATSU P5587 photo reflector is used to detect the colour change of the encoder wheel when it rotates. The pulses produced by the photo reflectors give the amount of rotation of the driving wheels

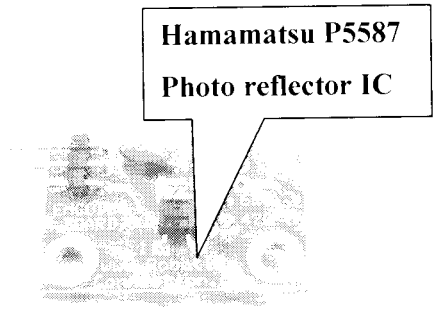

Figure 4-9 P5587 IR photo reflector module

Figure 4.9 shows the small PCB with the photo reflector used to produce the pulses with the wheel rotation. The photo reflector IC Hamamatsu P5587 is used as the main component in this PCB.

Figure 4-10 shows the attachment of the photo reflector module to the fiber platter. This should attach as close as possible to the encoder wheel. A proper identification of the white and black lines on the encoder can be done when the photo reflector is very much close to the encoder wheel.

Figure 4-10 Photo reflector module mounted near the DC servo motor

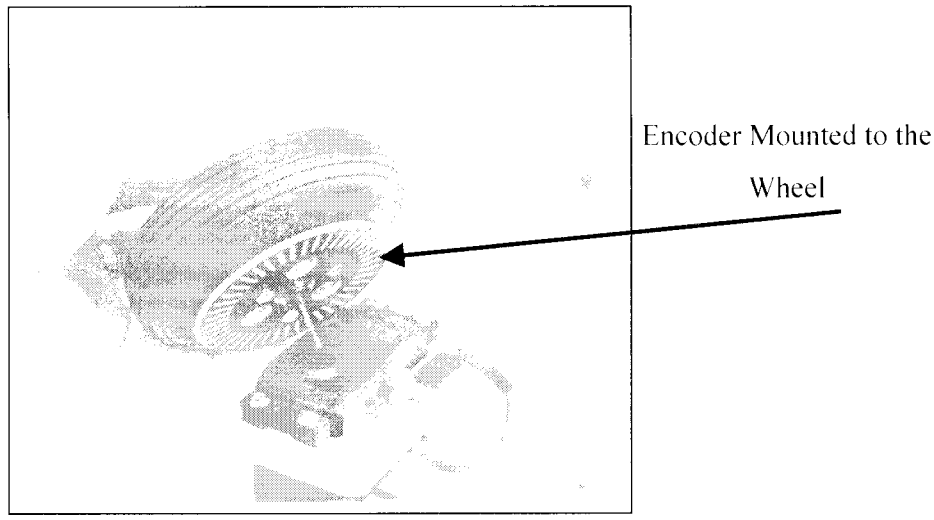

Figure 4-11 . Mounting the encoder unit to the servo motor unit

Figure 4.11 shows the encoder wheel screwed to the driving wheel. The driving wheel connects to the DC servo motor using a screw which passes through the hole in the center of the wheel.

4.6 The main controller

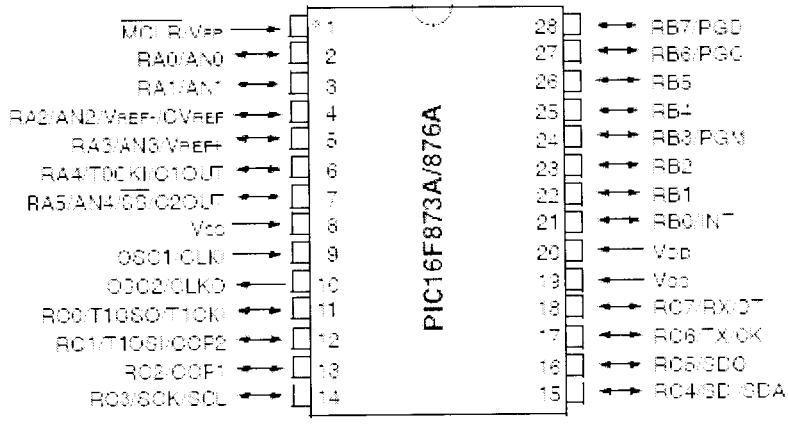

Figure 4-12 PIC16F876A microcontroller

The microcontroller PIC 16F876A is shows in fig.4-12.This microcontroller was developer by Microchip Inc.[16] and it is used as the main controller for this mobile robot. This microcontroller drives the two DC servo motors using its PWM modules. The Port B change interrupt detection facility of this microcontroller is used to reads the optical encoder outputs and establishes the communication between the computer software interface and the MR through the Universal asynchronous receiver and transmitter module (USART).The Pic Simulator IDE [23] developed by Oshon Software is used to developed the firmware for the PIC microcontroller. This firmware is written using the language called Pic basic.

4.7 RS232 communication between PIC and the PC

Software interface is developed using the visual basic software to control the MR and get data from the MR. This software provides the manual controlling facility of the robot as well. The positive width information sends by the microcontroller through the RS232 interface port of the computer is received and write those data to an excel file. The real time data viewing facility is available in this software and hence the object touching point and the data output of the MR can be observed.

4.8 The pusher

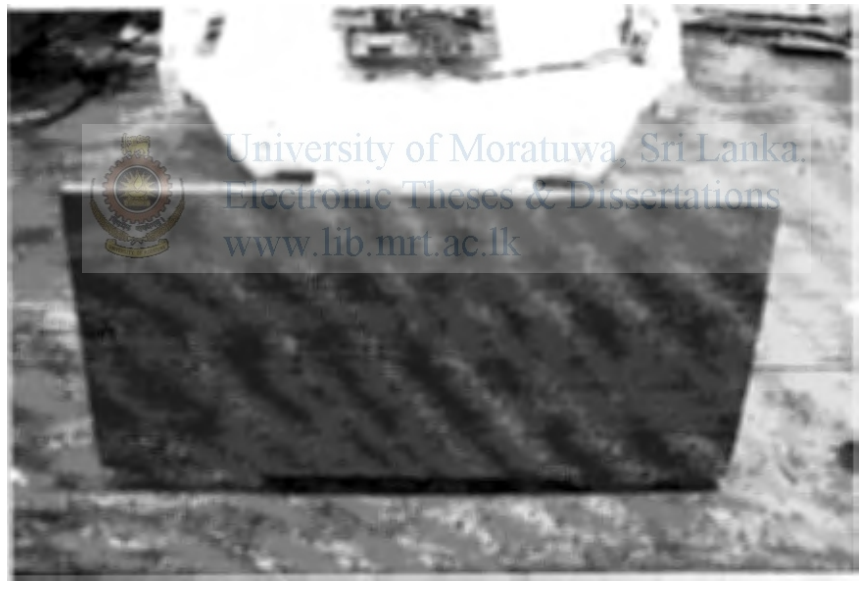

Figure 4-13. The object pushing plate attached to the Mobile Robot

The pusher is made out of 7mm MDF sheet. This is mounted in front of the MR as shown in figure 4-13.The middle line of this plate is called centre of pusher (COP). The geometrically symmetric plane of the MR passes through this COP. The COF of the pushing object should lie on this geometrically symmetric plane to get equal force

for the both left and right motors of the robot. This pushing plate creates force on the object and hence the friction of the object and the plate determines the amount of slip of the object along the pushing plate.

4.9 Basic block diagram of the mobile robot control circuit

The basic block diagram of the controller circuit is shown in Figure 4-14.The PWM frequency converter circuit block is the 250Hz to 50Hz PWM waveform converter. The 12^{th} and the 13^{th} pins of the PIC16F876A PIC microcontroller out the 250Hz PWM waveforms required to drive the motors and the converter module out the 50Hz PWM waveform. Left and the right motors encoder outputs are fed to the microcontroller via the 4rt and 5^{th} pins of the portB. The microcontroller can configure to detect the portB changes and it will create an interrupt when there is a value change in the portB. Hence it is easy to detect the number of pulses produced by both encoders. Since the white colour grooves on black background generates the encoder pulses, false pulses may generate due to dust or any other dark particles which stuck on the white groves of the encoder. So that the PIC microcontroller is program to double check the portB pin with a delay at every port change interrupt. This algorithm helps to omit the encoder pulses with short widths which generated by the dark particles on the white grooves.

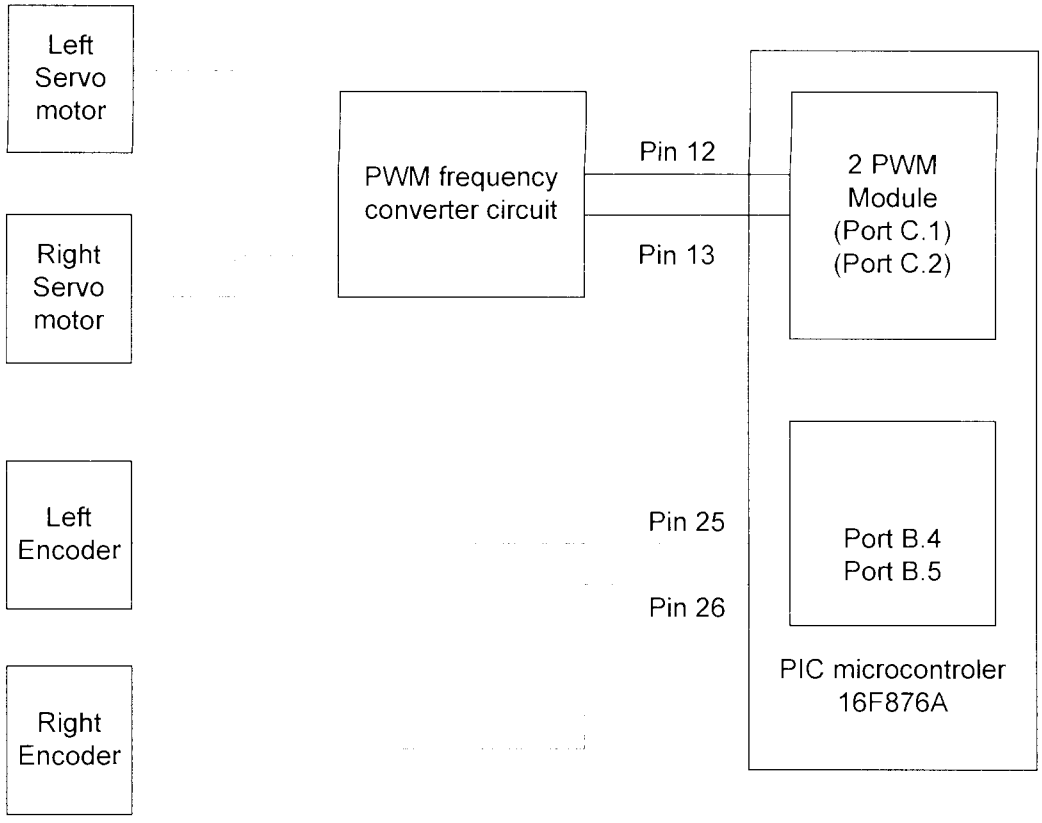

Figure 4-14: Block diagram of the controller circuit

4.10 The DC servo motor driving algorithm

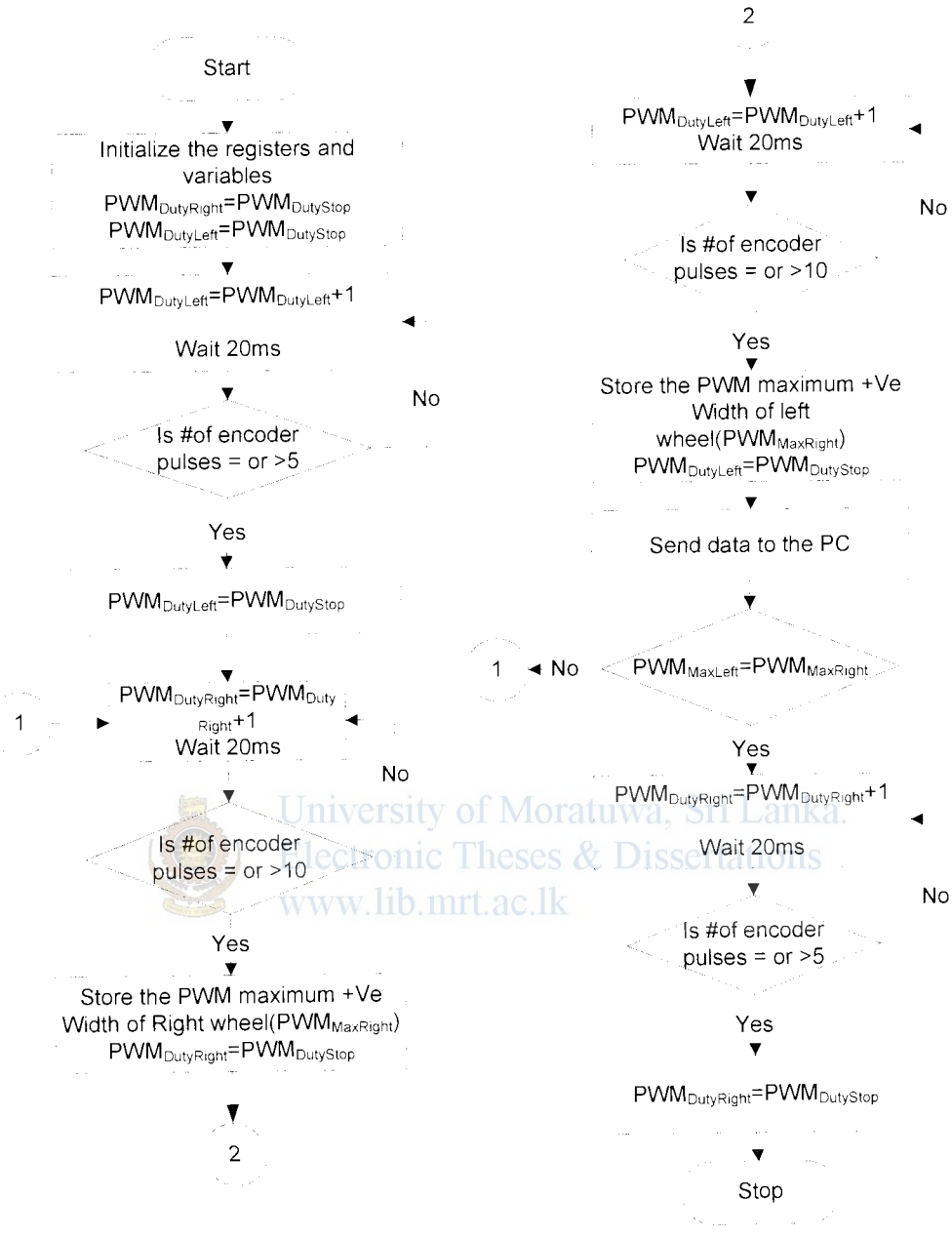

Figure 4-15 Flow chart of the robot controlling algorithm

Figure 4-15 shows the algorithm used to control the MR when it pushes an object. This algorithm is developed to test the object position and the positive width of the PWM signal. When robot detects equal positive pulse width from both motors the robot will turn to the middle of the object and stop its movement. Since the data sends

to the personal computer (PC) it is possible to store the motor driving pulse width information on the PC.

At the beginning of the movement of the MR it moves an angle which is equal to half of the full angle the robot rotate in normal pushing operation. So that at the beginning it can be observed that MR turns the motor until it detects 5 encoder pulses from the Right wheel encoder. For normal pushing operation the wheel rotate until the encoder produces 10 pulses. At the end of the operation MR turns the left wheel until it detects 5 encoder pulses. This movement helps to keep the MR in the same orientation at the begging and end of the pushing operation.

5 Results and Analysis

The main objective of this research is to detect the COF of the pushing object and align it to the centre of the pusher. So the object is kept in several places of the pusher, the MR operated until it detects equal measurements for both motors while it pushes the object in zigzag motion. The time taken to detect the COF of the object depends on several parameters listed below.

- Shape and mass distribution of the object.
- Friction between the terrain and the object.
- Friction between the terrain and the MR
- The amount of rotation of the pusher with the zigzag motion of the robot.
- The starting point of touch of the object with the pusher.

If the shape of the object is symmetrical and easy to push then the COF of the object comes to the centre of the pusher much quicker.

5.1 Test 1: Effect on positive PWM width and the steady state object position

Test 1 is performed using a cylindrical object made out of cement and a rectangular cuboid shaped battery. The weight of the cylindrical object is 950g and the diameter of the circular face is 15cm and the height is 9.5cm.Both cylindrical and rectangular cuboid shaped objects were kept at different positions of the pusher at the starting of the MR movement. The Figures 5-1 to Figure 5-6 shows the variation of final PWM positive width value of the robot motors in zigzag motion when the first touching point of the cylindrical object varies along the pusher. In all the charts we can see that

the robot is trying to make both motor driving duty cycles to an equal value. As we know that only when the pushing force is applied from equal distances away from the center of the pusher, it creates equal force in both side movements of the robot. So it is clear that the force created by the two motors become equal. So the firmware for the robot is developed to stop its movement once it detects same positive widths for both motors. Then the touching positions of the object and the pusher is measured using a ruler attached to the pusher.

It can be clearly seen that when the weight of the object changes, then the PWM positive width also changes accordingly. When the object is close to the edge of pusher, the motor attached to that side needs a considerably higher torque to drive the motor. So the positive pulse width becomes higher than the positive pulse width of the other side motor. This is a very good indication to prove the concept that is going to be examined in this research.

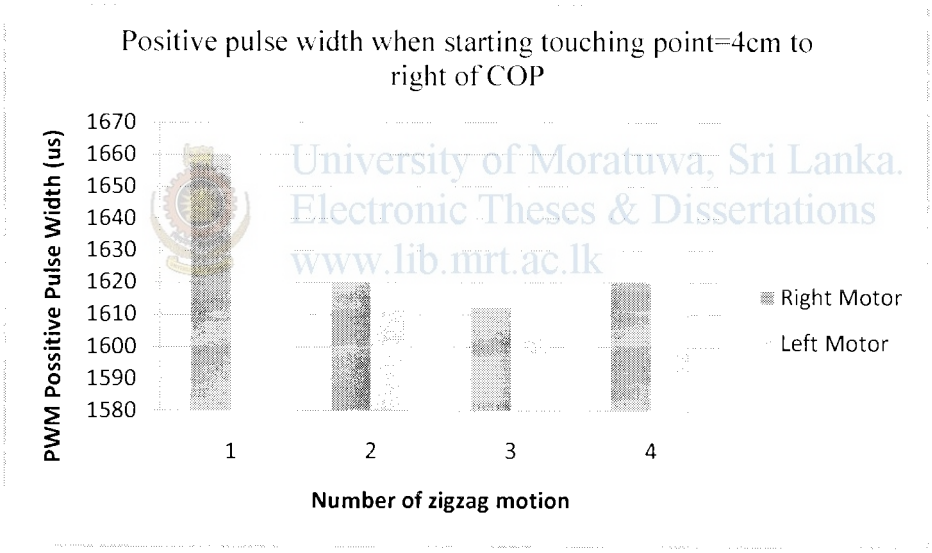

Figure 5-1: Motor driving positive width when the object is kept 4 cm to the right of the COP

Figure 5-1 shows the positive width variation of the zigzag motion when the cylindrical object touches the pusher on the left hand side. The initial touching point is 4cm from the left edge of the pusher. At the first pushing the object might not touch the pusher well and hence sudden impact occurs between the pusher and the object. This might lead to higher positive width to drive the motor.

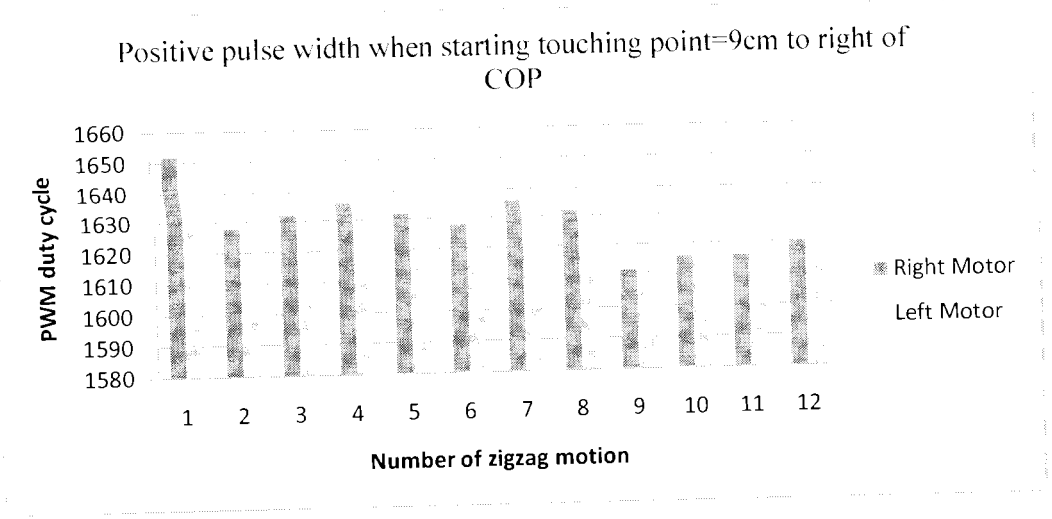

Figure 5-2: Motor driving positive width when the object is kept 9 cm to the right of the COP

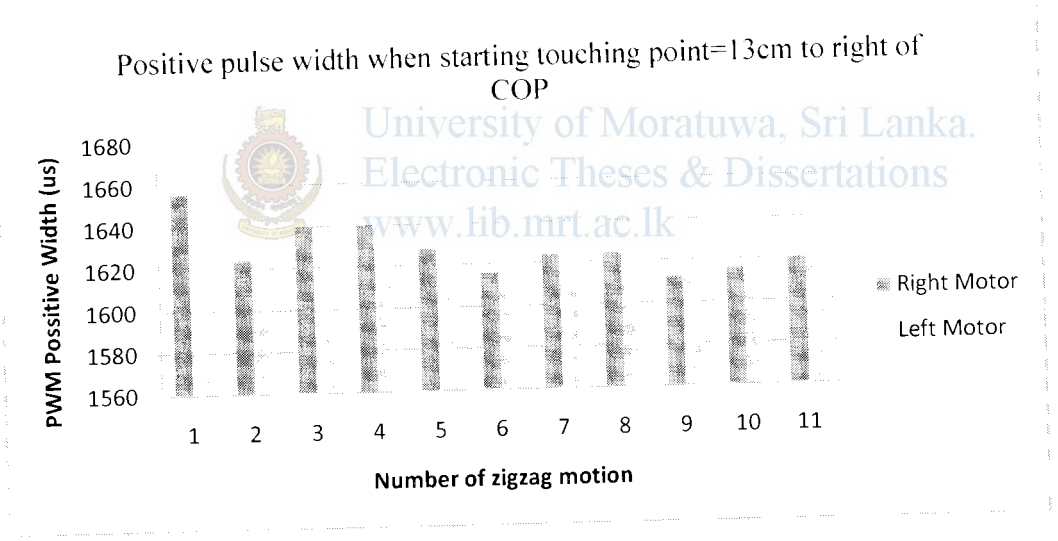

Figure 5-3: Motor driving positive width when the object is kept 13 cm to the right of the COP

Figure 5.3 shows the positive width variation when the first contact point of the pusher and the object is 13cm to the right of the centre of the pusher. It can be clearly observed that the positive pulse width of the right side motor movement is very much higher than that of the left motor at the beginning of the movement. This is because the object touches the pusher at the right corner of the pusher and the right motor has to push the object a long distance. So it will take more time to push the object and

hence the motor creates much higher torque. Because of the zigzag movement the object comes towards the pusher and hence difference of the positive widths of both motors becomes less.

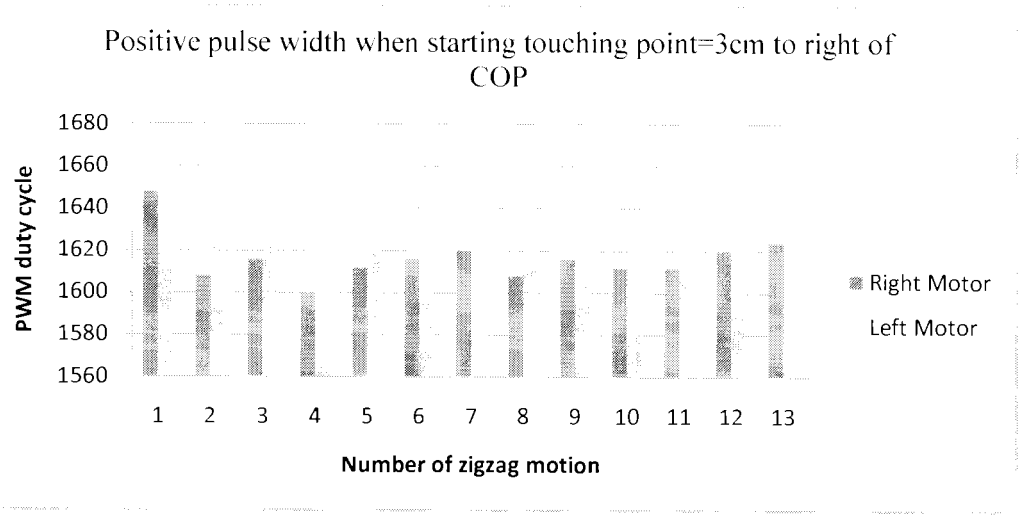

Figure 5-4: Motor driving positive width when the object is kept 3cm to the right of the COP

If the object is kept close to the centre of the pusher as shown in figure 5-4 the motor driving positive width difference of both left and right motors is not very high at the starting of the movement.

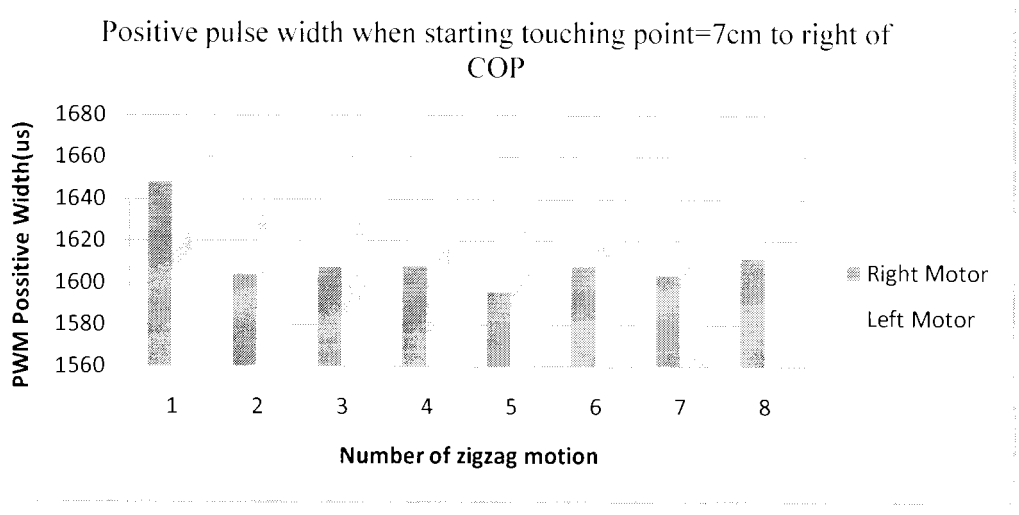

Figure 5-5: Motor driving positive width when the object is kept 7cm to the right of the COP

Though the object kept at different distances from the centre of the pusher the motor driving positive width might not show significant difference at the starting. This is due to the initial touching point of the object and the pusher. At some orientations of the pusher and the object the pusher might turn the object and will not push the object very much. Turning around the COF needs less force than pushing through the COF. So motor torque needed to turn an object is less than the torque needsed to push an object through the COF. In some of these results this phenomenon can be observed.

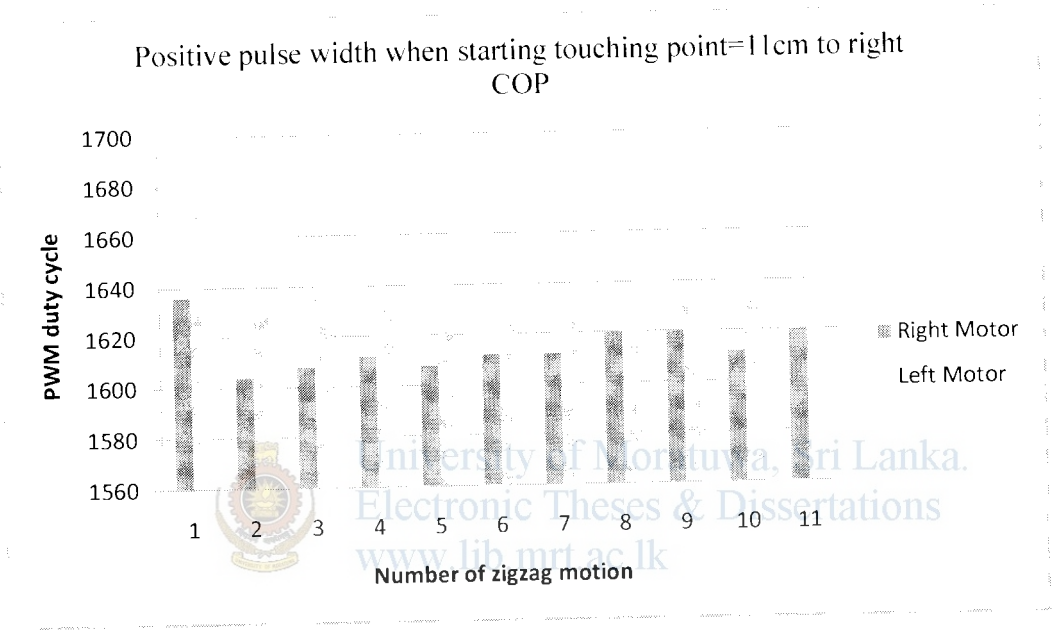

Figure 5-6:Motor driving positive width when the object is kept 11cm to the right of the COP

It can be clearly seen that when the object is kept at the left side of the pusher the left motor needs more torque than the right and vice versa. Hence

Figure 5.7 and 5.8 shows the measurements of the final touching point deviation from the centre of the pusher when both motor driving duty cycles become equal for cylindrical and rectangular cuboid shaped objects respectively. The starting touching point of the object varies along the pusher to get several final touching points

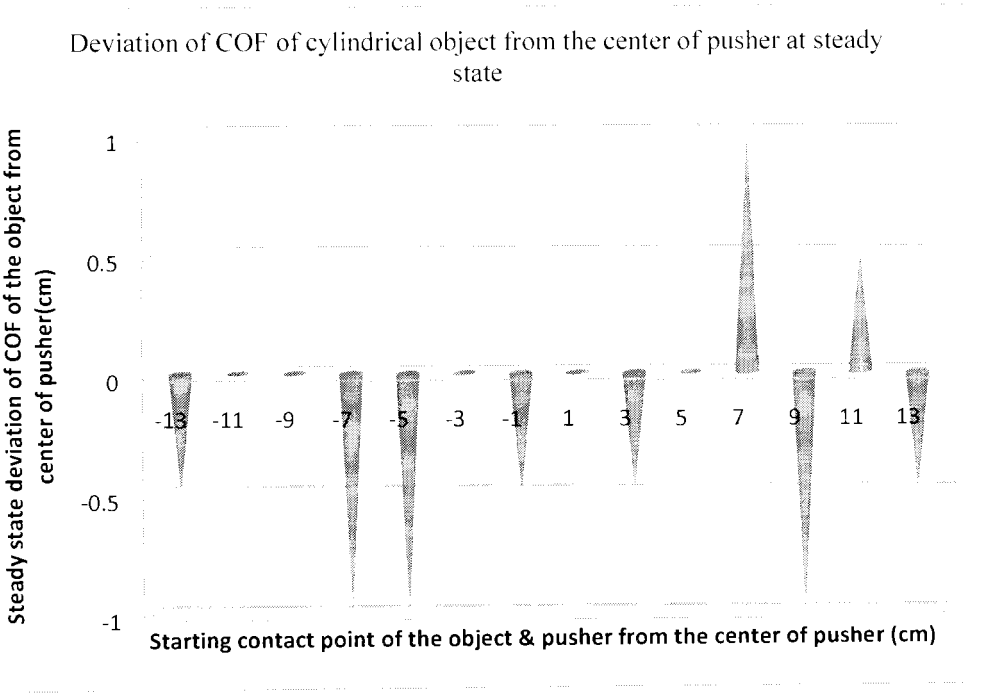

Figure 5-7: Deviation of the COF of a cylindrical shaped object from the center of pusher at steady state.

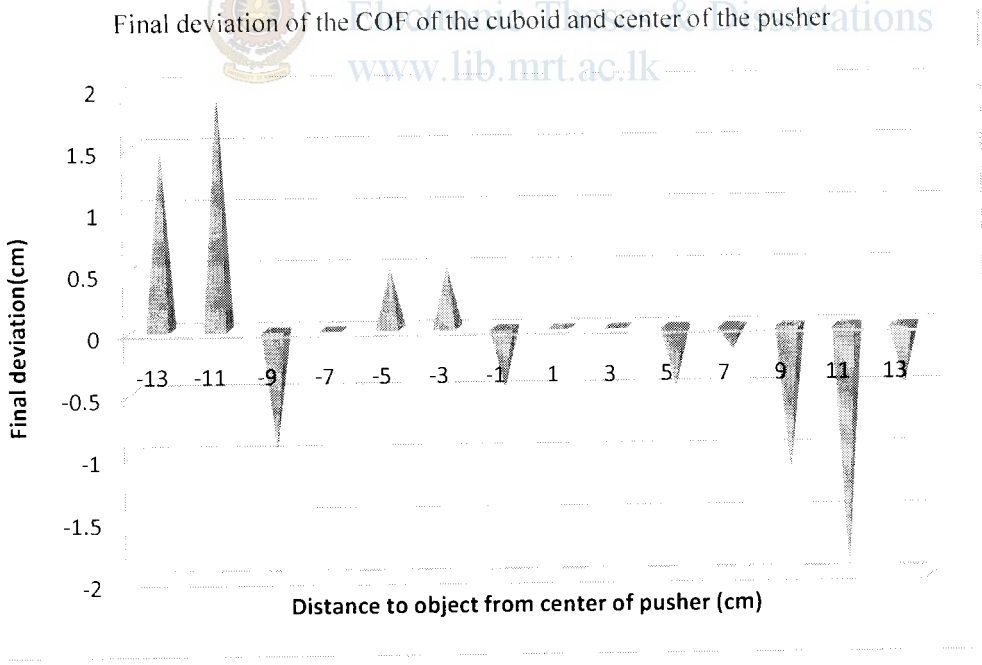

Figure 5-8: Deviation of the COF of a rectangular cuboid shaped object from the center of the pusher at steady state.

For the cylindrical object the maximum deviation of the real centre of friction of the object and the centre of the pusher is in ±1 cm. The above mentioned deviation for the rectangular cuboid is in ±2cm .So it is clear that this method can be effectively used to find the centre of friction of an object.Instead of the above feature this zigzag motion is a very effective method to move any shaped object to the centre of the pusher. This will help to keep the pushing object close to the centre of the pusher all the time that the robot pushes the object.

5.2 Test 2: Effect on the terrain and weight of the object

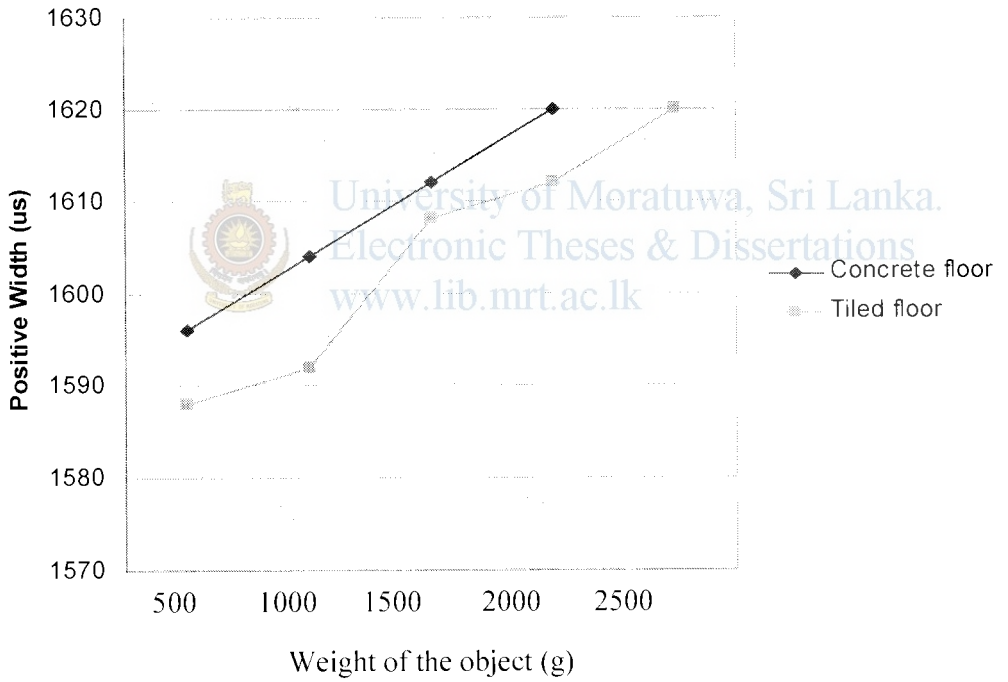

Figure 5-9: The effect on positive pulse width when the weight of the object changed

The second test was performed to find the effect on the positive width of the PWM value when the weight of the object is changed. This test was done for both tiled floor and a concrete floor. A five liter water bottle was used as the object in this test. This

bottle was filled with 500ml of water and the first test performed in a tiled floor and got the PWM width at the force balance state. The same test was done by adding 500ml extra water each and every time and got the readings. Figure 5-9 shows the result of the above test. It is difficult to go for higher weights with the existing MR. When the weight increases the wheels start to slip and hence it is hard to go for higher weights. On a concrete floor the result is very much linear than on a tiled floor. This is because the MR may slip on a tiled floor. This slipping may cause an error on the result.

Figure 5-10 shows how the mobile robot pushes the piece of granite with an odd shape. The positive width values of each and every movement of the robot are shown under the images. Here the robot has turned due to the slip. Though it is turned it has no effect on the final result. Finally the object and the pusher got aligned and the positive width values become equal.

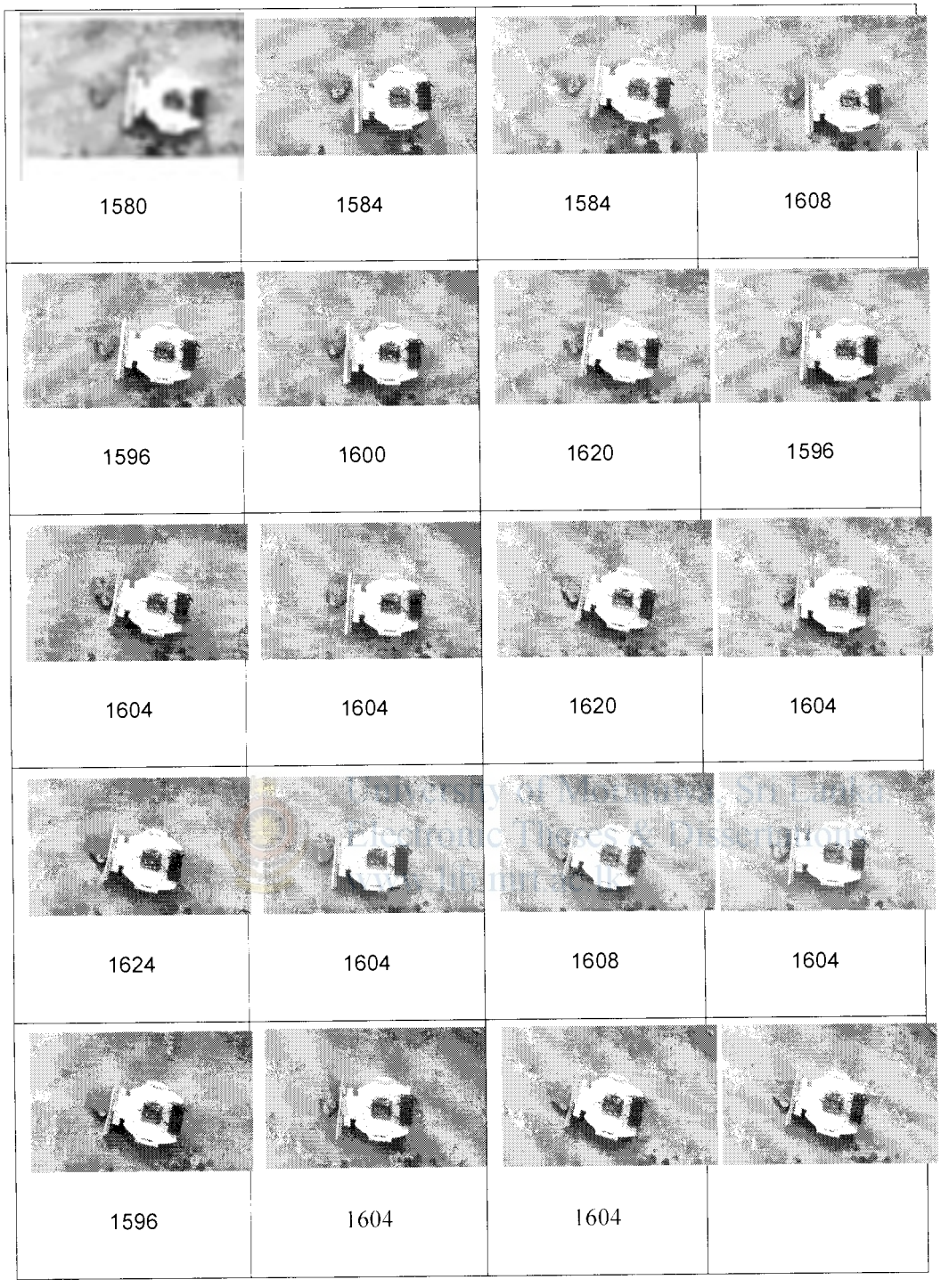

Figure 5-10 Robot pushing a piece of granite

Chapter 6

6 Conclusion and Recommendation

The torque created by a motor is a good measurement to detect the external force applied to it. The motor torque of a DC servo motor can be changed by changing the duty cycle of the PWM waveform which drives the motor. A MR with two wheels attached to two DC servo motors, it is possible to detect the reaction on both wheels when it drives independently. If the MR moves in a horizontal plane with no obstacles, reaction on both wheels will be equal if the weight distribution of the robot is symmetrical. If there is an obstacle which creates the reaction force on the MR through the symmetrical axis then also equal reaction force creates on both wheels. Only difference is that the reaction force is having a higher value than the obstacle free motion. But when an object creates a reaction force on the MR breaking the above symmetry it will lead to a different reaction force on both wheels. It tends to different driving torques on both motors.

With the positive width of the motor driving PWM wave and the encoder pulses created by wheel rotation it is possible to detect the point of the pusher which the reaction of the pushing object passes through. Since this process is done using one motor at a time the robot creates a zigzag moment. This zigzag moment is helped to push the object towards the centre of the pusher and hence the object does not try to go away from the pusher. This is a great advantage when pushing an object.

The most important thing in this process is that it utilizes only the wheel encoder pulses and the properties of the motor driving PWM waveform. No other sensor is used in this technique and hence this is a very low cost effective solution for object pushing robots.

There is another very valuable output in this technique. This method can be used with any shaped object which can be moved either by rolling or sliding. Most of the previous researches were limited to either a box or a cylinder shaped object. It is hard to find the center of mass of an object using most of the other techniques, if the mass

distribution of the object is uneven. But in this method the object turns and pushed towards the centre of the pusher until the pusher gets the same reaction from both sides pushing in a zigzag motion. At this instance the geometrical centre of the object is not important. The reaction created through the centre of friction of the object is measured by this technique.

Since the friction of the terrain equally affects both the MR and the object the MR should have enough weight to create a sufficient friction when it pushes objects with larger weight. The wheels also should create sufficient friction to push the object. Hence the robot can designed with fairly thick tires.

There are some other ways to detect the force applied on the motor much accurately than the technique used in this research. Some other techniques like "Disturbance observer" will improve the bandwidth of the force detection created by the motor. Using this technique the motor driving force can be determined with higher accuracy. Then the COF of the object can be aligned with the centre of the pusher more accurately than the result obtained in this technique.

This robot is designed to push any object which contacts the pusher when it is moving. Using a camera or an ultrasound sensor the robot will be able to find the position of the objects and then the MR can move towards the object. If the sensors can identify the Geometrical center of the object then the center of the pusher and the geometrical center of the object can get aligned in it's first contact. This will help to minimize the number of zigzag movements to detect the COF.

The amount of rotation of the MR in this zigzag motion can be optimized. Hence it is possible to do the job faster and save the energy. This will be another research area in the future. At the end of the COF of the object and the center of the pusher alignment, MR need not undergo the zigzag movement. Then the robot can move the object to the target with the normal motion. If there is any movement of the object detected along the pusher while it is pushing with normal motion, the zigzag motion can apply to correct the COF and the center of pusher deviation.

By adding some robot navigation technique it is possible to develop this MR to push an object to a predefined target. GPS navigation techniques can be used for outdoor applications. Landmark-based, map-based, vision based positioning or localisation can

be used for indoor or outdoor navigations. Then the robot can be used for applications such as cleaning corridors, pushing granite blocks in a quarry etc.

References

[1]. Mason, M.T., "Mechanics and planning of manipulator pushing operations". International Journal of Robotics Research, vol**5(3)**: 53-71, Fall. 1986.

[2]. R. C. Brost. "Automatic grasp planning in the presence of uncertainty". International Journal of Robotics Research, Vol.7, No.1, February 1988.

[3]. M. Mani and W. Wilson. "A programmable orienting system far at parts". North American Manufacturing Research Institute Conference XIII, 1985

[4]. Peshkin M.A., Sanderson A.C., "The motion of a pushed, sliding work piece", IEEE J. on Robotic. & Automation., vol.4(6):569-598, 1988.

[5]. M. A. Peshkin and A. C. Sanderson. "Planning robotic manipulation strategies for work pieces that slide". IEEE Journal of Robotics and Automation, Vol.4, No.5, October 1988.

[6]. Akella Srinivas and M.T. Mason. Posing polygonal objects in the plane by pushing. In IEEE International Conference on Robotics and Automation, pages 2255-2262 ,1992.

[7]. Akella S., Mason M.T.," Parts orienting by push-aligning", *IEEE Int'l Conf. on Rob. & Autom. ICRA '95*, , Nagoya, Japan vol.1:414-420,May 1995.

[8]. Lynch, Kevin M., Hitoshi Maekawa, and Kazuo Tanie, "Manipulation and active sensing by pushing using tactile feedback". Proceedings of theIEEE/RSJ International Conference on Intelligent Robots and Systems, pages 416-421,1992.

[9]. Agarwal, Pankaj K., Jean-Claude Latombe, Prabhakar Raghavan and Rajeev Motwani. "Nonholonomic path planning for pushing a disk among obstacles". Proceedings of IEEE International Conference on Robotics and Automation. 1997.

[10]. Takagi, Seiji and Yoshikuni Okawa." Rule- based control of a mobile robot for the push-a-box Operation". Proceedings of IEEE/RSJ International Workshop on Intelligent Robots and System ,1991.

[11]. Okawa, Yoshikuni and Ken Yokoyama. Control of a mobile robot for the push-a-box Operation. In proceedings of IEEE International Conference on Robotics and Automation, 1992.

[12]. Lynch, Kevin M. Nonprehensile robotic manipulation: controllability and planning. PhD thesis, Robotics Institute, Carnegie Mello University, Pittsburg, Pennsylvania, 1996.

[13]. Seiichiro Katsura, Kouhei Irie, and Kiyoshi Ohishi, Wideband Force Control by Position-Acceleration Integrated Disturbance Observer,IEEE Transactions on Industrial Electronics, VOL. 55, NO. 4, April 2008

[14]. S. Katsura, Y. Matsumoto, and K. Ohnishi, "Analysis and experimental validation of force bandwidth for force control," *IEEE Trans. Ind. Electron.*, vol. 53, no. 3, pp. 922–928, Jun. 2006.

[15]. S. Katsura, Y. Matsumoto, and K. Ohnishi, "Modeling of force sensing and validation of disturbance observer for force control," *IEEE Transaction on Industrial Electronics.*, vol. 54, no. 1, pp. 530–538, Feb. 2007.

[16]. Microchip Technology Inc.,PIC16F87XA datasheet(DS30582B),pp2,2003

[17]. Fairchild Semiconductor Corporation,DM74LS08,Quad 2 input and gate datasheet(DS006347), 2000

[18]. Peshkin, Michael A., and Arthur C. Sanderson. The motion of a pushed, sliding workpiece. IEEE Journal of Robotics and Automation, 4(6), 569-598. 1988a.

[19]. Peshkin, Michael A. and Arthur C. Sanderson. Planning robotic manipulation strategies for work pieces that slide. IEEE Journal of Robotics and Automation, 4(5), 524- 531. 1988b

[20]. Mathtthew T. Mason, Mechanics of Robotics Manipulation, Prentice-hall of India, pp 121-141, 2005

[21]. SGS THOMPSON microelectronics corporation,HCF4017 datasheet, June1989.

[22]. A.M.H.S. Abeykoon, Kouhei Ohnishi, "Estimation of Optimal Slip for Traction Force Improvement of a Mobile Manipulator", Proceedings of the International Conference on Information and Automation, Colombo, Sri Lanka, December, 2005,.

[23]. http://www.oshonsoft.com/

[24]. Wang, Yu and M.T. Mason. Two-Dimensional Rigid-Body Collisions With Friction. Journal of Applied Mechanics Vol.60, June, pp. 566. 1993.

[25]. De Wit, C.C., B. Siciliano, and G. Bstin. Theory of Robot control, Springer-Verlag, London. 1996.

6.1 Appendix A: Source code for testing robot

The source code written for the PIC BASIC compiler is given below

```
Hseropen 9600
Dim duty1 As Word
Dim duty2 As Word
Dim duty1_temp As Word
Dim duty2_temp As Word
Dim preinput1 As Bit
Dim preinput2 As Bit
Dim x As Bit
Dim pulse_1 As Word
Dim pulse_2 As Word
Dim pulse As Word
Dim drive As Byte
Dim duty_st As Word
Dim duty_th As Word

duty_st = 375
duty_th = 385
duty1 = duty_st
duty2 = duty_st


pulse_1 = 0
pulse_2 = 0
trisb.4 = 1
trisb.5 = 1

INTCON.GIE = 1  'enable all un-masked interrupts
INTCON.PEIE = 1  'enable pheripheral un-masked interrupts
```

```
INTCON.rbie = 1  'ENABLE PORTB CHANGE INTERRUPT
PIE1.rcie = 1

PWMon 1, 1
PWMon 2, 1
pr2 = 249
PWMduty 1, duty1
PWMduty 2, duty2

preinput1 = portb.4
preinput2 = portb.5
drive = "F"


loop0:
        If pulse_2 <= 5 Then
                duty2 = duty2 + 1
                PWMduty 2, duty2
                WaitMs 100
                Goto loop0
        Else
                PWMduty 2, duty_st
                pulse_2 = 0
        Endif

main:
If drive = "F" Then
        loop1:
        If pulse_1 <= 10 Then
                duty1 = duty1 + 1
                PWMduty 1, duty1
                WaitMs 100
                Goto loop1
        Endif
```

```
If pulse_1 > 10 Then
        PWMduty 1, duty_st
        Hserout "R", #duty1, " "
        duty1_temp = duty1
        duty1 = duty_st
        pulse_1 = 0
Endif

loop2:
If pulse_2 <= 10 Then
        duty2 = duty2 + 1
        PWMduty 2, duty2
        WaitMs 100
        Goto loop2
Endif

If pulse_2 > 10 Then
        PWMduty 2, duty_st
        Hserout "L", #duty2, CrLf
        duty2_temp = duty2
        duty2 = duty_st
        pulse_2 = 0
Endif


If duty1_temp > duty_th And duty2_temp > duty_th Then
        If duty1_temp = duty2_temp Then
                loop3:
                        If pulse_1 <= 5 Then
                                duty1 = duty1 + 1
                                PWMduty 1, duty1
                                WaitMs 100
                                Goto loop3
```

```
                    Else
                        pulse_1 = 0
                    Endif

                PWMduty 1, 400
                PWMduty 2, 400
                WaitMs 3000
            Endif
        Endif
Else

            PWMduty 1, duty_st
            PWMduty 2, duty_st

Endif
Goto main
End
```



```
On Interrupt
Save System
If PIR1.rcif = 1 Then
            Hserin drive
Endif

If INTCON.rbif = 1 Then
        x = Not preinput1
        If portb.4 = x Then
            pulse_1 = pulse_1 + 1
            preinput1 = portb.4
        Endif
        x = Not preinput2
        If portb.5 = x Then
            pulse_2 = pulse_2 + 1
```

```
            preinput2 = portb.5
        Endif

        INTCON.rbif = 0
Endif

Resume
```